REQ. NO. 0-9021

CONTRACT REPORT NO. OSU80-00223

FINAL REPORT FOR EMR CONTRACT

20SU-23440-0-9021

on

Development of a Technique for Contact Angle Measurements on Irregularly Shaped Solid Particles

Continuing Work of UP-T-96

Principal Investigator: Dr. A.W. Neumann

April, 1981

University of Toronto
Department of Mechanical Engineering
5 King's College Road
Toronto, Ontario
M5S 1A4

104 pp

JUL 20 1981
MICROMEDIA

TABLE OF CONTENTS

Page

INTRODUCTION.....1

EXPERIMENTAL MATERIALS

1. Coal Samples.....3
2. Matrix Materials.....4

RESULTS AND DISCUSSION

1. Level 1 "Ranking" Procedure.....5
2. Level 2 Critical Velocity Measurements.....5
3. Other Physical Characteristics of the Coal Samples
   - 3.1 Moisture Content.....7
   - 3.2 Specific Heat.....8
   - 3.3 Neutron Activation Analysis of Coal.....9

SUMMARY OF CONCLUSIONS.....11

DESIGN OF A NEW SOLIDIFICATION CELL.....12

TABLES 1-7.....14-20

FIGURES 1-4.....21-24

APPENDIX No.1. Contact Angle Measurements on Coal Particles from Solidification Front Experiments

APPENDIX No.2. Wettability of Coal Particles: Contact Angle Measurements from Solidification Front Experiments

APPENDIX No.3. Temperature Dependent Specific Heats of Polymers by Differential Scanning Calorimetry

INTRODUCTION

This work is the continuation of the EMR Contract DSS 07SU-23440-9-9046. The purpose of this investigation was to develop a novel technique for the characterization of surface properties of coal powders.

The natural hydrophobicity of coal is different for coals of different origin (of different rank). The particle/vapour interfacial tension, γ_{PV}, as well as the contact angle with water, θ, on coal can be used to characterize the hydrophobicity and hence the floatability of the coal powders.

Contact angle measurements are difficult to perform with any powder. However, the "freezing front technique", recently developed in our laboratory, has been proven to be a good method for the determination of the surface parameters of small particles. The method interprets quantitatively engulfment or rejection of the particles by the solidification front of suitably chosen matrix materials.

During the previous contract period in 1979/80 an investigation of two bituminous and one subbituminous coal samples from different origins was initiated. The studies of these samples were augmented and the measurements refined to such an extent that the results are now publishable. Three manuscripts containing this information are appended (Appendix 1, 2 and 3). In addition, 4 new bituminous coal samples were investigated, again on both levels of the freezing front technique.

The approach adopted has two levels:

1) The first level consists of the "ranking" of the coal samples by comparing, in effect, the particle surface tension,

γ_{PV}, with the surface tension, γ_{LV}, of the matrix materials used in the experiments.

2) The second level of the investigation involves the determination of the critical velocity of engulfing, V_c. This critical velocity can be correlated with the free energy of adhesion (ΔF^{adh}), the various surface tensions and contact angles on coal by dimensional analysis. For more details on the experimental set-up and the method see Appendices No. 1 and No. 2.

MATERIALS AND METHODS

1. Coal Samples

We studied four medium volatile bituminous coal samples (CN-1, CN-2, CN-3A and CN-5A) from British Columbia (Crownest Pass Area, Alberta – B.C. border). These samples were dry screened after grinding and were provided by EMR, CANMET Western Research Laboratory, Edmonton. Each of the coal samples consists of two fractions identified by a range of -60+100 and -200+325 mesh, respectively.

Our microscopic measurement showed that the -60+100 mesh fractions have particles with a mean diameter of approximately 200 μm, while the -200+325 mesh fractions have a wide distribution in size (in the range of approximate by 45-90 μm in diameter) with a mean diameter of 70 μm. The larger particles are covered with a layer of very small (of the order of 1-5 μm in diameter) particles.

One aliquot part of each sample was oven-dried at 105°C. All of the experiments were performed with both the original and the oven-dried samples.

Another aliquot part of the coal samples was exposed to glow discharge to check whether this treatment renders the surface of the coal particles more hydrophilic due to oxidation of the surface layer.

The results for another medium volatile bituminous coal, sample No. 2 from the former measurements are also used in comparison with the present results. This sample was wet screened after grinding and consists of six mesh fractions.

The origin of coal No. 2 is Mountain Park Area, near Hinton, Alberta.

2. Matrix Materials

The matrix materials used were thymol, biphenyl, naphthalene, phenyl salicylate (salol) and 2-phenyl phenol. All of the matrices were zone refined prior to the measurements.

The physical and thermal properties of the matrix materials are summarized in Table 1.

RESULTS AND DISCUSSION

1. Level 1 "Ranking" Procedure

In level 1 all the coal samples (all the different fractions) were rejected by the solidification front of the different matrix materials at relatively low solidification rates. This means that the particle/vapour interfacial tension, γ_{PV}, is higher than the highest value of liquid/vapour interfacial tension, γ_{LV}, of the matrix material used, which happens to be 2-phenyl phenol, with a surface tension of γ_{LV} = 38.7 mJ/m^2 at 59°C (41.3 mJ/m^2 at 20°C).

2. Level 2 Critical Velocity Measurements

In level 2 the critical velocity of engulfment, V_c, was determined for the coal samples with thymol as matrix material.

The drying time of the samples at 105°C and the exposure time of particles to glow discharge were also varied prior to the experiment. The samples were oven-dried for 24 and 72 hours, respectively, or were exposed to glow discharge for 15 and 30 minutes, respectively, after drying them for 72 hours at 105°C. The aim of these investigations was to check the influence of the variation of the experimental circumstances on the reproducibility of critical velocity values. There were no significant differences in critical velocities after the treatments. It means that the samples have relatively low moisture content (see Table 4), which might not influence the critical velocity determination. In the other case we suppose that the surface of the samples were either oxidized already or the glow discharge does not affect them.

The critical velocity, free energy of adhesion (ΔF^{adh}) and the particle/vapour interfacial tension values of the coal samples (including No. 2) are summarized in Table 2 for thymol at the melting temperature of thymol (at 51.5°C). These critical velocity values are the mean values of at least 30 measurements. From the critical velocity measurements we have been able to estimate an average temperature coefficient of particle surface tension as $\frac{d\gamma_{PV}}{dT} = -0.065[mJ/m^2 \cdot K]$ (see Appendix No. 1). In Table 3 the particle surface tensions, γ_{PV}, and the contact angles with water, θ, calculated by using this average temperature coefficient of γ_{PV} are given for 20°C.

The γ_{PV} and contact angle versus particle diameter, D, for thymol as matrix material are plotted in Figs. 1 and 2 for the five coal samples. The solid line refers to coal sample No. 2 for which a number of particle sizes were investigated. For the other 4 coal samples (CN-1, CN-2, CN-3A and CN-5A) only 2 particle sizes (70 and 200 μm in diameter) were investigated; the data points are connected by dotted lines. The particle/vapour interfacial tension, γ_{PV}, of the coal samples increases, the contact angle with water, θ, decreases with increasing particle size (with decreasing mesh size) in all cases.

The hydrophobicity of the coal samples considered here increases in the following order (cf. Figs. 1 and 2): CN-5A < CN<2 < CN-3A < CN-1 $\leq$ No. 2. The range of wettability for the four types of particles is relatively small. This was expected, as the samples are all medium volatile bituminous coal from the same area.

3. Other Physical Characteristics of the Coal Samples

Various physical properties of the coal samples such as density, moisture and ash content, surface area and specific heat for each fraction were determined experimentally and are summarized in Table 4. In the Tables 4-7, the coal samples are arranged in the order of decreasing hydrophobicity. From the results summarized here, it is clear that there is no strong correlation, if any, between the hydrophobicity and the other physical properties investigated. The density, surface area and ash content were measured in the Western Research Laboratory, CANMET, Edmonton, moisture content and the specific heat measurements were performed in our laboratory.

3.1 Moisture Content [wt %]

The moisture content of the samples was determined by measuring the loss of weight by heating to a temperature slightly higher than the boiling point of water. Coal powder (0.2 - 0.5 g) in weighing bottles was oven-dried at 105°C until the weight of the sample remained constant. After cooling in a desiccator, the loss of weight was determined with analytical accuracy. The mean values of the moisture content of each original coal sample are given in Table 4.

It should be noted that these bituminous coal samples have very low moisture content (almost all of them less than 1%) and they differ only slightly from each other. That fact makes it plausible why no differences were found in the behaviour of the original and oven-dried samples.

3.2 Specific Heat [kJ/(kg·K)]

The specific heat, C_p, of the coal samples was determined by Differential Scanning Calorimetry (DSC). The heating rate was chosen as 10 K/min, the chart speed as 20 mm/min, chart range as 5 mV. The reference standard was a sapphire disc (α - $A\ell_2O_3$) and the $A\ell_2O_3$ specific heat data used for calibration were obtained from the work of Ginnings and Furukawa (see Appendix No. 3, Ref. 9). All measurements were carried out in an atmosphere of flowing N_2 gas over a temperature range of 300 to 360 K. Since data for comparison were not available for coal powders, it was also decided to measure the specific heats of several polymeric materials. For more details see Appendix No. 3.

The C_p values in Table 4 were used for the calculation of ΔF^{adh}; they refer to the melting temperature of thymol as matrix material.

The temperature dependence of specific heats of the original and oven-dried samples are summarized in Table 5 for -60+100 mesh and in Table 6 for -200+325 mesh fractions, respectively. The errors given in Table 5 and 6 are 95 percent confidence limits. The specific heat values are plotted as a function of temperature for the original, untreated and for the oven-dried samples of both fractions in Figs. 1 and 2, respectively.

The specific heat of coal samples increases with increasing temperature. The untreated -60+100 fractions (Fig. 1) show S-type curves with increasing temperature, while C_p for the oven-dried samples changes linearly. This difference of behaviour

between dried and untreated coal is more pronounced in the case of higher moisture content of the untreated samples.

The C_p-temperature curves of dried and untreated coal samples for the smaller particle size (-200+325 mesh, Fig. 2) show similar character; neither the linear function for the dried samples nor the S-curve for the untreated samples is as pronounced as it was in the case of the larger (-60+100) mesh fraction. The coal samples with smaller particle size have lower moisture content than the corresponding fractions with larger mesh size (Table 4). The drying process does not effect the specific heats considerably. Coal sample No. CN-1 has the highest specific heat value. The specific heats, C_p, of the other samples are somewhat smaller but indistinguishable from each other in the error limits.

3.3 Neutron Activation Analysis (NAA) of Coal

The mineral composition of the coal samples was determined by means of neutron activation analysis using the University of Toronto's SLOWPOKE reactor.

This analysis was performed at 5 kW and/or 2 kW flux for 20 and/or 22 minutes/g, respectively. The coal standard reference was SMR 1632 from the U.S. National Bureau of Standards, Washington D.C. The results are summarized in Table 7 for 12 elements. The concentration of the elements is given in percent or ppm, respectively, and the error given represents the 95 percent confidence limits. No differences were found between the untreated and dried samples as far as cation-contamination is concerned, but there was a difference in the concentration of

the two anions (Cℓ, Br). Therefore one datum is given for each element in the case of cations in Table 7, but two ppm values are given for the chlorine and bromine contamination. The chlorine and bromine contents are higher in the original, untreated samples. The negative charge of the anions might influence the zeta potential of the coal particles and may be relevant in the processing.

No correlation between inorganic contamination and hydrophobic character of the coal samples is apparent. In general, CN-1 coal is least contaminated and CN-5A, i.e. the most hydrophilic coal, is the coal with the highest contamination. Otherwise, there is no correspondence between contamination and hydrophobicity.

The coal samples examined here have extremely low sodium (Na) content and somewhat higher titanium (Ti) and dysprosium (Dy) content than the standard sample.

SUMMARY OF CONCLUSIONS

1) The physical characteristics of the four bituminous coal samples examined during the present contract period are similar to each other which might be expected for coal powders from the same origin. These samples do not show significant differences from the bituminous coal No. 2 either.

2) However, the critical velocity measurements show a small, but definite, difference in surface characteristics between the four samples.

3) Overall there is little difference between the four coal samples CN-1, CN-2, CN-3A and CN-5A. It is only the high sensitivity of the freezing front technique which shows distinct, although small differences between the samples.

DESIGN OF A NEW SOLIDIFICATION CELL

The experimental apparatus for the freezing front experiments is similar to the one used by S.N. Omenyi (see Ref. 13 in Appendix No. 1). It consists of a copper cell in which the measurements are made. A temperature gradient is imposed on the matrix material by maintaining a temperature gradient in the copper. The temperature of the matrix material is lowered, and therefore the solidification front caused to move, by lowering the temperature of the copper.

The chamber is heated electrically at one end and cooled by circulating water through a copper tube at the other end of the cell. If the heat transfer area between the cell and the cooling coil is larger, a better response of the solidification front velocity to change in water temperature is obtained. That was the reason why a new solidification cell was designed with thermoelectric heating and cooling.

The temperature control has been improved over the previous apparatus. The temperature of the copper, and therefore the matrix material, is varied by heating or cooling by means of thermoelectric devices at each end of the copper cell. The temperature at each end is independently controlled by a feedback controller. Both the temperature difference between the two ends, and therefore the temperature gradient, and the rate of change of temperature are controlled.

The velocity of the solidification front is varied by varying the temperature gradient and the rate of change of the temperature of the copper cell. The temperature gradient and

the rate of change of temperature are selected by means of digital potentiometers in the controller. This allows much easier control of the velocity than the previous apparatus. The velocity is well controlled and can be reproduced. Furthermore the temperature gradient can now be controlled.

TABLE 1

THERMAL AND PHYSICAL PROPERTIES OF ORGANIC MATRIX MATERIALS

SUBSTANCE	DENSITY [kg/m^3]	VISCOSITY [$N \cdot s/m^2$]	SPECIFIC HEAT [$kJ/kg \cdot K$]	THERMAL CONDUCTIVITY [$J/(m \cdot s \cdot K)$]	SURFACE TENSION, γ_{LV}, at melting point [mJ/m^2]
THYMOL	925	0.00397	2.370	0.1298	29.9 at 51.5°C
BIPHENYL	992	0.00149	1.842	0.1424	32.5 at 70°C
NAPHTHALENE	978	0.000967	1.683	0.2261	32.8 at 80°C
SALOL	1200	0.00889	1.637	0.0837	35.3 at 43°C
2-PHENYL PHENOL	1210				38.7 at 59°C

TABLE 2
CRITICAL VELOCITY, ΔF^{adh} AND γ_{PV} DATA
FROM EXPERIMENTAL OBSERVATIONS WITH
THYMOL AT 51.5°C

Samples	COAL FRACTIONS AT 51.5°C					
	-60+100 mesh			-200+325 mesh		
	Critical Velocity V_c [μm/sec]	ΔF^{adh} [mJ/m²]	γ_{PV} [mJ/m²]	Critical Velocity V_c [μm/sec]	ΔF^{adh} [mJ/m²]	γ_{PV} [mJ/m²]
No. 2	5.7±1.6	0.169±0.032	42.0±2.3	8.1±2.6	0.130±0.029	39.1±2.1
CN-1	6.0±2.5	0.181±0.053	42.8±3.8	8.5±1.0	0.133±0.011	39.4±0.8
CN-3A	7.0±1.5	0.201±0.030	44.2±2.1	11.5±1.5	0.166±0.015	41.7±1.1
CN-2	7.5±2.0	0.212±0.039	45.0±2.9	13.5±2.0	0.182±0.019	42.9±1.4
CN-5A	9.5±1.0	0.247±0.022	47.5±1.6	14.0±2.0	0.188±0.018	43.3±1.3

TABLE 3

PARTICLE/VAPOUR INTERFACIAL TENSION AND CONTACT ANGLE DATA OF COAL SAMPLES AT 20°C

Sample	γ_{PV} at 20°C [mJ/m^2]		θ at 20°C [degrees]	
	-60+100 mesh	-200+325 mesh	-60+100 mesh	-200+325 mesh
No. 2	44.0±2.3	41.2±2.1	65.6±3.9	70.4±3.5
CN-1	44.9±2.8	41.5±0.8	64.2±3.4	69.9±1.3
CN-3A	46.3±2.1	43.8±1.1	61.7±3.6	66.0±1.9
CN-2	47.1±2.9	45.0±1.4	60.4±3.7	64.0±2.4
CN-5A	49.6±1.6	45.4±1.3	56.2±2.7	63.3±2.2

TABLE 4

PHYSICAL PROPERTIES OF COAL SAMPLES

Physical Properties	COAL SAMPLES									
	-60+100 mesh					-200+325 mesh				
	No. 2	CN-1	CN-3A	CN-2	CN-5A	No. 2	CN-1	CN-3A	CN-2	CN-5A
DENSITY* [kg/m^3]	1470	1340	1390	1350	1410	1430	1440	1460	1560	1460
MOISTURE CONTENT [wt%]	0.47	1.08	1.13	0.73	0.71	0.64	0.46	0.66	0.53	0.51
ASH CONTENT* [wt%]	13.33	8.69	13.04	10.03	14.70	17.03	8.26	16.25	10.10	14.89
SURFACE AREA* [m^2/kg]	620	610	520	830	900	890	1080	1220	1910	1090
SPECIFIC HEAT at 51.5°C [kJ/(kg·K)]	1.12	1.16	1.13	1.14	1.14	1.19	1.30	1.21	1.24	1.25

*These data were obtained from EMR, CANMET, Western Research Laboratories, Edmonton, Alta., courtesy of Dr. H. Hamza.

TABLE 5

TEMPERATURE DEPENDENCE OF SPECIFIC HEATS OF THE ORIGINAL AND OVEN-DRIED COAL SAMPLES (-60+100 mesh fractions)

Temperature K	Specific Heat C_p(kJ/kg·K)							
	original		-60+100 mesh		dried		-60+100 mesh	
	CN-1	CN-3A	CN-2A	CN-5A	CN-1	CN-3A	CN-2A	CN-5A
300	1.07±0.05	1.07±0.04	1.07±0.06	1.05±0.00	1.17±0.01	1.08±0.02	1.12±0.19	1.09±0.03
310	1.11±0.02	1.09±0.04	1.10±0.01	1.10±0.04	1.24±0.10	1.14±0.04	1.16±0.01	1.14±0.02
320	1.14±0.01	1.10±0.04	1.12±0.01	1.12±0.05	1.24±0.16	1.15±0.00	1.18±0.01	1.14±0.02
330	1.17±0.09	1.16±0.00	1.17±0.02	1.15±0.04	1.28±0.12	1.17±0.01	1.21±0.01	1.18±0.07
340	1.25±0.10	1.22±0.08	1.21±0.11	1.17±0.13	1.31±0.13	1.20±0.00	1.22±0.01	1.21±0.07
350	1.35±0.09	1.26±0.05	1.23±0.03	1.23±0.04	1.32±0.14	1.22±0.06	1.24±0.04	1.21±0.06
360	1.37±0.06	1.31±0.01	1.27±0.04	1.26±0.06	1.38±0.01	1.24±0.18	1.29±0.03	1.24±0.01

TABLE 6

TEMPERATURE DEPENDENCE OF SPECIFIC HEATS OF
THE ORIGINAL AND OVEN-DRIED COAL SAMPLES
(-200+325 mesh fractions)

Temperature	Specific Heat C_p(kJ/kg·K)							
K	original		-200+325 mesh		dried		-200+325 mesh	
	CN-1	CN-3A	CN-2A	CN-5A	CN-1	CN-3A	CN-2A	CN-5A
300	1.13±0.07	1.09±0.09	1.10±0.10	1.08±0.03	1.07±0.10	1.10±0.09	1.11±0.07	1.11±0.10
310	1.24±0.17	1.18±0.03	1.20±0.04	1.18±0.06	1.17±0.08	1.15±0.11	1.22±0.05	1.13±0.08
320	1.28±0.21	1.19±0.07	1.23±0.06	1.23±0.06	1.20±0.12	1.19±0.08	1.25±0.11	1.18±0.06
330	1.33±0.19	1.24±0.07	1.28±0.04	1.27±0.05	1.26±0.14	1.24±0.07	1.30±0.14	1.25±0.08
340	1.38±0.21	1.29±0.07	1.31±0.07	1.29±0.06	1.31±0.08	1.27±0.08	1.34±0.12	1.29±0.14
350	1.43±0.14	1.33±0.14	1.34±0.08	1.32±0.07	1.36±0.15	1.30±0.10	1.39±0.22	1.33±0.04
360	1.46±0.18	1.37±0.17	1.38±0.06	1.39±0.18	1.39±0.16	1.34±0.14	1.41±0.13	1.36±0.10

TABLE 7

MINERAL CONTAMINATION OF COAL SAMPLES

BY NEUTRON ACTIVATION ANALYSIS

Element	-60+100 mesh				-200+325 mesh				NSB-SRH
[ppm]	CN-1	CN-3A	CN-2	CN-5A	CN-1	CN-3A	CN-2	CN-5A	Standard Coal
Al wt %	1.42±0.02	1.91±0.13	1.65±0.04	2.35±0.06	1.39±0.09	2.04±0.07	1.64±0.03	2.18±0.01	1.51±0.08
Ca wt %	0.07±0.01	0.11±0.02	0.09±0.01	0.03±0.01	0.09±0.02	0.13±0.02	0.10±0.01	0.06±0.01	0.37±0.04
Mg wt %	0.27±0.01	0.39±0.03	0.33±0.01	0.45±0.03	0.26±0.01	0.44±0.02	0.33±0.01	0.44±0.02	0.19±0.04
Na wt %	0.005±0.001	0.009±0.001	0.007±0.001	0.008±0.001	0.006±0.001	0.010±0.001	0.011±0.001	0.009±0.001	0.036±0.002
Ba	79±14	89±11	93±7	105±9	141±14	110±7	126±11	180±4	320±20
Ti	1200±46	1449±72	1387±40	1883±51	1176±63	1529±51	1404±33	1888±72	920±50
V	36.1±1.6	54.3±3.1	45.4±1.1	47.9±1.3	37.2±1.7	60.7±2.9	47.6±1.4	51.5±2.7	32.3±1.5
Mn	15.9±1.4	4.3±0.6	17.3±1.9	3.3±0.2	18.4±1.4	6.4±0.2	11.3±0.8	7.7±0.2	41±2
U	1.2±0.1	1.6±0.1	1.4±0.1	1.6±0.1	1.3±0.2	1.9±0.07	1.5±0.0	1.7±0.0	1.6±0.2
Dy	1.16±0.04	1.57±0.07	1.38±0.07	1.49±0.04	1.16±0.02	1.71±0.04	1.32±0.05	1.56±0.04	0.57±0.04
Cl orig. / dried	187±1 / 63±1	71±1 / 70±3	205±4 / 124±2	115±12 / 64±1	304±4 / 117±20	108±4 / 88±10	304±1 / 158±7	210±9 / 100±14	920±30
Br orig. / dried	53.5±2.2 / 47.2±0.3	24.0±0.1 / 17.6±1.3	78.0±0.6 / 59.0±1.2	53.1±0.5 / 36.2±0.6	110±2 / 108±5	68±1 / 58±2	167±1 / 140±1	137±4 / 112±1	16.6±0.6

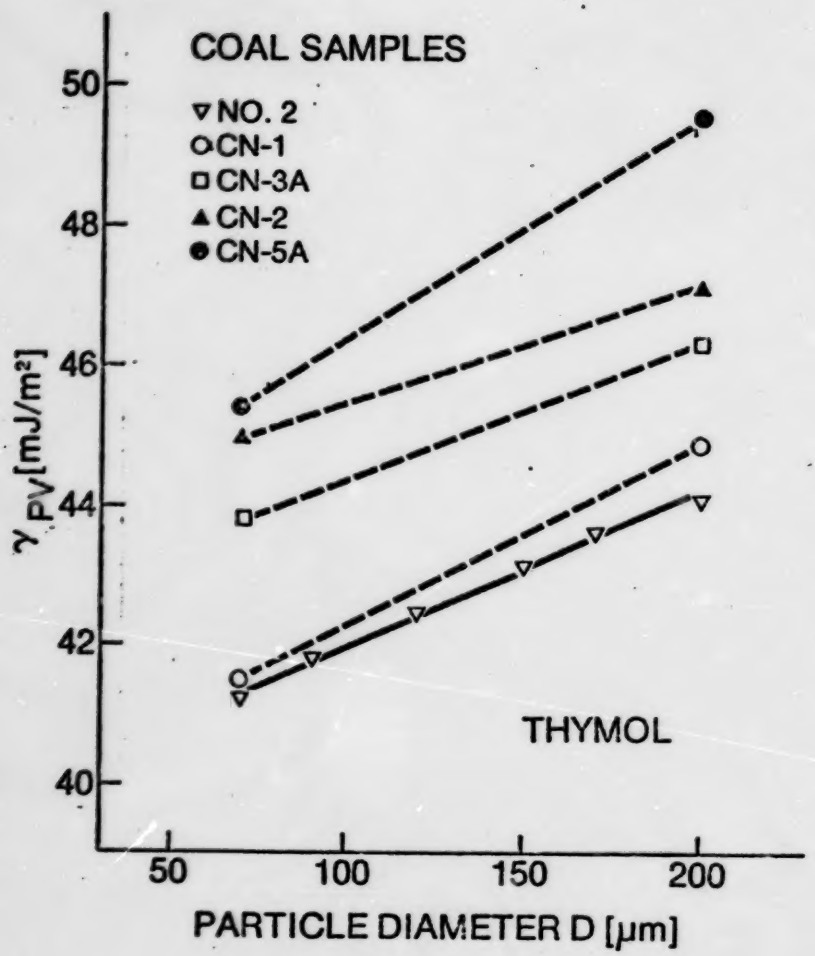

Figure 1. Particle/Vapour Interfacial Tension, γ_{PV}, vs. Particle Diameter, D

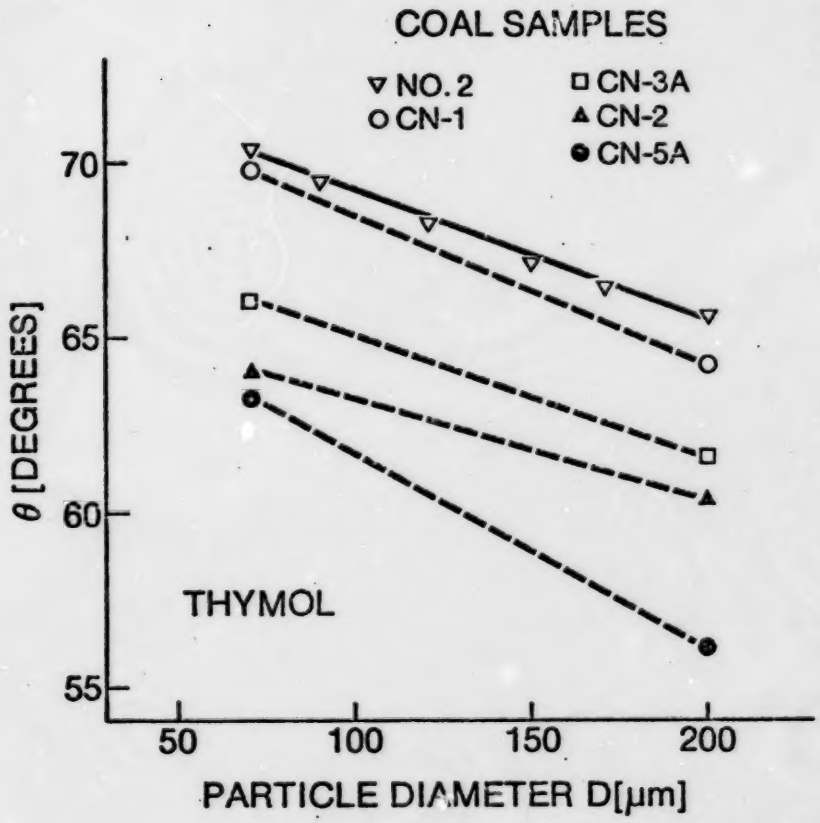

Figure 2. Contact Angle with Water, θ, vs. Particle Diameter, D

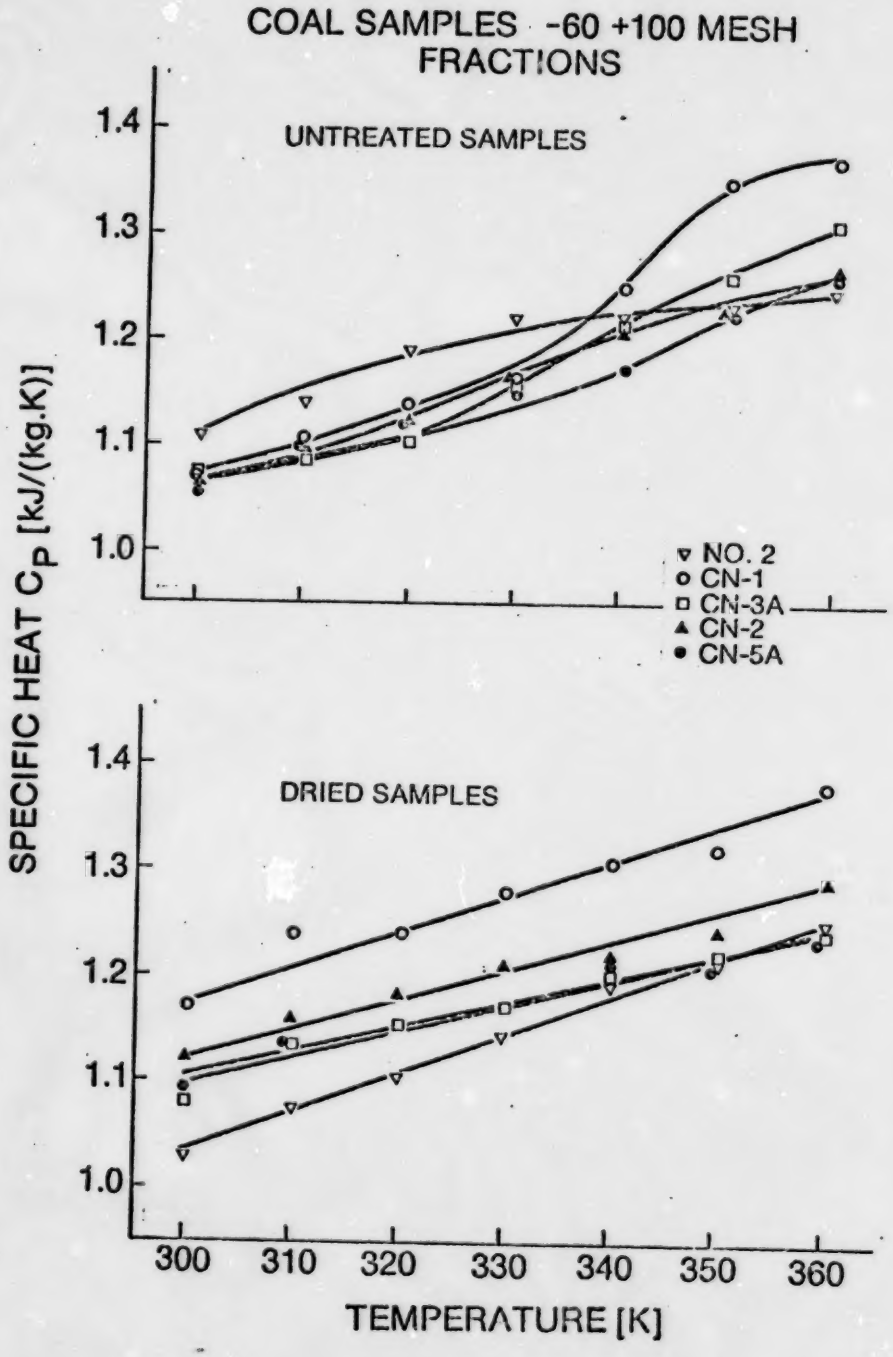

Figure 3. Temperature Dependence of Specific Heats for -60+100 Mesh Fractions

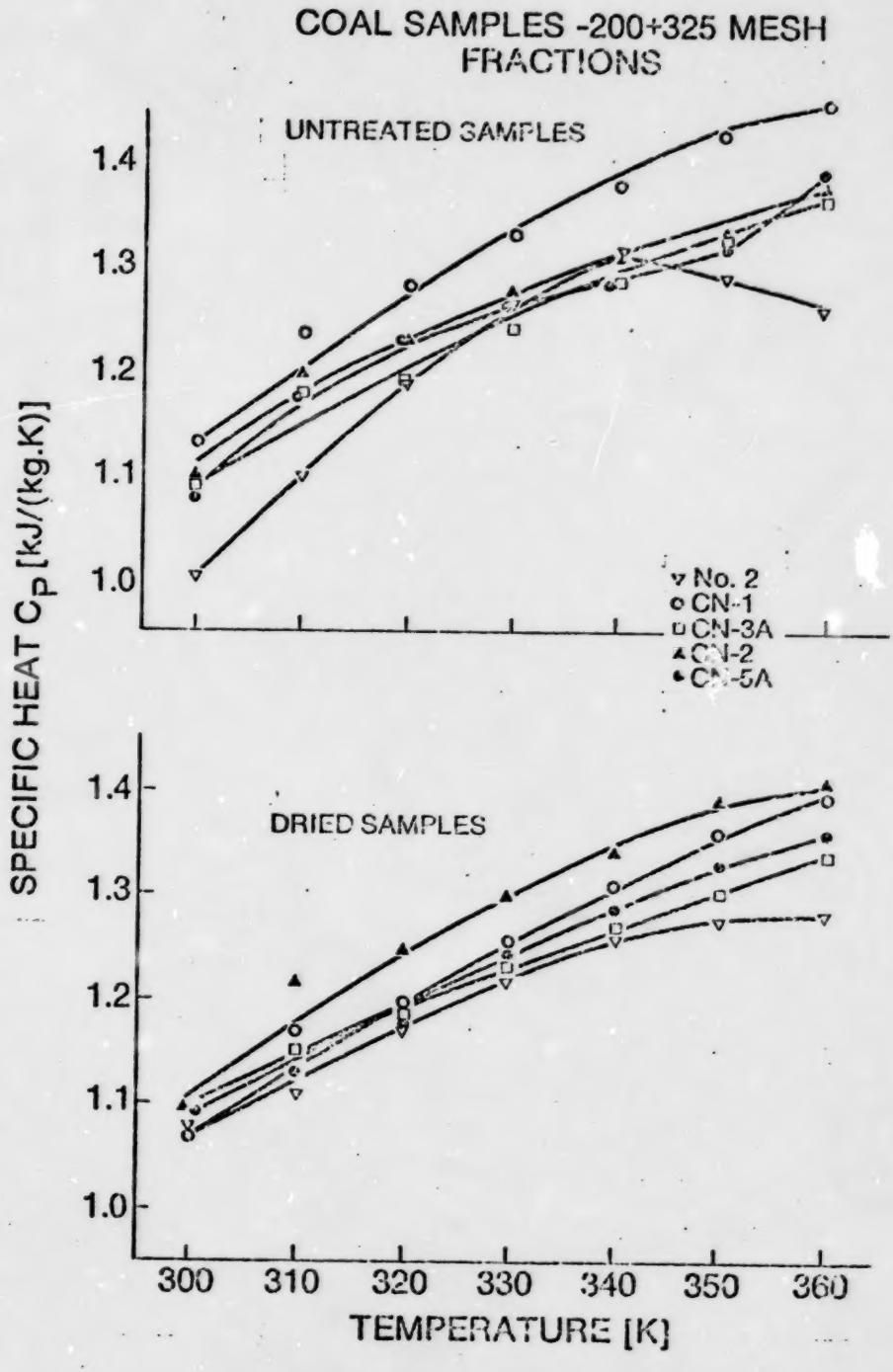

Figure 4. Temperature Dependence of Specific Heats for -200+325 Mesh Fractions

APPENDIX No.1

CONTACT ANGLE MEASUREMENTS ON COAL PARTICLES FROM SOLIDIFICATION FRONT EXPERIMENTS

E.I. Vargha-Butler*, M.R. Soulard*, H. Hamza+ and A.W. Neumann*

* University of Toronto
Department of Mechanical Engineering
Toronto, Ontario, Canada

+ EMR, Western Research Laboratory, CANMET
Edmonton, Alberta, Canada

INTRODUCTION

The surface tension and the contact angle of small, irregularly shaped coal particles play an important role in various energy resources related processes such as froth flotation of coal powders or coal-oil mixtures.

It was found that a contact angle of above 60-65 degrees with distilled water is required for good floatability (1,2). It was also recognized that the wettability of coal depends on its carbon content (2,3) and is influenced by ash content and mineral contamination. The higher the ash content the less hydrophobic is the sample (4).

Earlier contact angle measurements were performed with bulk coal samples or with particles mounted in a matrix material and polished. One of the first reviews of various methods of contact angle measurements on coal was given by BRADY and GAUGER (5). The authors discussed the sessile drop method which provides a direct measurement of contact angles from drop profiles. The contact angle, θ, may be either determined using a telescope equipped with a goniometer eyepiece or from a photograph. For more details on this method see Ref. (6).

The captive bubble method introduced by TAGGART, TAYLOR and INCE (7) has been extensively applied by a number of investigators in connection with coal flotation studies (1,3,5,8,9). The contact angle may be measured by means of a protractor on an enlarged image of the gas bubble adhering at the solid/liquid interface.

The tilting plate method which was devised by ADAM and JESSOP (10) has also been applied to the study of coal

wettability (11,12). A plate dips into a liquid which forms a concave or convex meniscus near the plate. The plate is tilted until the meniscus becomes horizontal; the angle between the plate and this horizontal is then taken as the contact angle. A more complete review of conventional contact angle methods is available in the literature (6).

From a review of the factors which might influence the value of the contact angle on coal, it was concluded that exposure of a coal surface to air often has unpredictable effects on its contact angle with water (5). In the case of coal surfaces considerable improvement in the measurement of contact angles resulted from the use of small gas bubbles rather than drops of liquid because the liquid droplets might be easier contaminated at the liquid/air interface (5).

Serious difficulties were encountered in obtaining test specimens of the necessary shape and dimensions especially for the tilting plate method.

According to HORSLEY and SMITH (3) one of the greatest difficulties in contact angle measurements on coal is the necessity of eliminating all traces of grease and other contaminants from the surface of the coal including traces of the polishing powder used in the preparation of the specimens. An attempt was made to verify that the contact angle, measured on bulk specimens or on compressed coal powder (after polishing the surface), is independent of the type of polishing cloth employed (3). But it was not proven that this contact angle value is really characteristic for the coal or coal particles as they exist in the beneficiation process (e.g. in flotation).

In our opinion the most important problem in connection with contact angles on coal particles was not discussed by any of the authors, namely, that the polished, pretreated coal surface is not identical with the original "natural" surface of coal. We want to emphasize that the characterization of the hydrophobicity of the coal samples by contact angles has to be done with coal powders after grinding and wet or dry screening, without any further treatment. The reason for the lack of such studies was not lack of insight, but lack of a technique which allows such contact angle measurements.

A novel technique for the measurement of contact angles on small particles has recently been developed and applied to the determination of contact angles on coal powders. This method interprets quantitatively engulfment or rejection of the coal particles by the solidification front of suitably chosen matrix materials.

THEORY AND METHOD OF SOLIDIFICATION FRONT EXPERIMENTS

At low solidification rates particles imbedded in a melt may be either rejected or engulfed when encountered by the solidification front. Thermodynamically, the free energy of engulfing (ΔF_{net}) of a particle by the solid phase is

$$\Delta F_{net} = \gamma_{PS} - \gamma_{PL} \qquad (1)$$

where

γ_{PS} = particle/solid interfacial tension;

γ_{PL} = particle/liquid interfacial tension.

Engulfment is expected when the free energy change as given in Eq. (1) is negative. If it is positive rejection is predicted.

The approach adopted has two levels:

Level 1: "Ranking" Procedure

Level 1 consists of the "ranking" of the coal samples in comparison with the liquid/vapour interfacial tension, γ_{LV}, of the matrix materials. With respect to the known interfacial tensions of the matrix materials used, there are two cases of interest:

1. The matrix material has a larger liquid/vapour interfacial tension, γ_{LV}, than the solid/vapour interfacial tension, γ_{SV}, i.e. $\gamma_{LV} > \gamma_{SV}$ for the matrix. In this case, if the particle/vapour interfacial tension, γ_{PV}, is less than the liquid/vapour interfacial tension of the matrix, γ_{LV}, engulfment occurs. If γ_{PV} is larger than γ_{LV}, the particle will be rejected. All of the matrix materials considered here belong to this category.
2. If we use a matrix with a solid/vapour interfacial tension, γ_{SV}, larger than the liquid/vapour interfacial tension, γ_{LV}, i.e. $\gamma_{SV} > \gamma_{LV}$, the conditions for particle engulfment or rejection are reversed. Water/ice is one example of this category (13).

For level 1 investigations one has to perform solidification front experiments with a number of matrix materials for all test particles at low solidification rates. If the particles are rejected by the solidification front of one of the matrix materials used, implying that $\gamma_{PV} > \gamma_{LV}$, the experiment will be repeated with the matrix material having the next higher γ_{LV}. If the particles are engulfed, i.e. $\gamma_{PV} < \gamma_{LV}$, the experiment should be

repeated with the matrix having the next lower γ_{LV}. In principle, the experiment will be continued using several matrix materials with different γ_{LV}, until the lower and upper bounds of the particle/ vapour interfacial tension, γ_{PV}, for the given coal sample can be determined.

For level 1 experiments a suitably chosen and large selection of matrix materials with different liquid/vapour interfacial tension, γ_{LV}, is desirable. Conditions for the selection of matrix materials will be discussed in the experimental section. This technique may be used in an analogous way to the float-sink experiments used to fractionate the coal according to its specific gravity. A liquid of intermediate density is used to separate the coal sample into a float fraction and a sink fraction. The latter is then fractionated in another liquid of higher density and so on. The information generated is the basis for the standard gravity washability curves which are used as a measure of how a coal is expected to behave in a gravity washing operation. In the case of the hydrophobicity by the engulfing technique similar washability curves may be constructed for those beneficiation processes dependent on surface character.

Level 2: Critical Velocity Measurements

The level 2 experiments involve the determination of the critical velocity of engulfment. At low rates of solidification all particles will be rejected, if $\gamma_{PV} > \gamma_{LV}$. As the rate of solidification increases, the hydrodynamic drag force opposing the particle motion will increase and at a certain rate, called critical velocity, V_c, the two forces become equal and engulfment

occurs. V_c can be determined experimentally and correlated with the interfacial free energy of adhesion (ΔF^{adh}) by means of a scheme of dimensional analysis (14,15). If the various physical properties both of particle and matrix materials are all known, ΔF^{adh} can be calculated from the experimental values of the critical velocity, V_c, using the following expression (16)

$$\Delta F^{adh} = 0.141\left[\frac{\rho_L^{0.6854}\ T_{MP}^{0.3995}}{\mu^{0.0849}}\right]\left[\frac{k_P^{0.6005}}{(\rho_P C_P)^{0.2009}}\right] D^{0.4844}\ V_c^{0.6854} \qquad (2)$$

where

$\Delta F^{adh} = \gamma_{PS} - \gamma_{PL} - \gamma_{SL}$, the free energy of adhesion [ergs/cm^2];

ρ_L = density of matrix material [g/cm^3];

μ = viscosity of matrix material [Poise];

ρ_P = density of particle [g/cm^3];

C_P = specific heat of particle [cal/(g·K)];

k_P = thermal conductivity of particle [cal/(sec·cm·K)];

T_{MP} = melting point of matrix material [K];

D = diameter of particle [μm];

V_c = critical velocity of particle engulfing [μm/sec].

The next step in the calculation is to determine the particle/vapour interfacial tension, γ_{PV}, for coal from the ΔF^{adh} value. Calibration curves of γ_{PV} vs. ΔF^{adh} are available for each matrix material considered here (15-17). The liquid/vapour surface tension, γ_{LV}, of the matrix materials can be easily determined by conventional techniques. γ_{PL} may be calculated from an equation of state relation (18,19)

$$\gamma_{PL} = \frac{[(\gamma_{PV})^{\frac{1}{2}} - (\gamma_{LV})^{\frac{1}{2}}]^2}{1 - 0.015(\gamma_{PV}\gamma_{LV})^{\frac{1}{2}}} \quad (3)$$

The contact angle with water, θ, on coal may then be calculated from Young's equation

$$\gamma_{PV} - \gamma_{PL} = \gamma_{LV} \cos\theta \quad (4)$$

By means of level 2 experiments, if the critical velocity is determined as a function of particle diameter, it is possible to determine a possible particle size dependence of the particle/vapour interfacial tension, γ_{PV}, and also a dependence of the contact angles, θ, of e.g. water, on coal particles.

EXPERIMENTAL

Apparatus

The experimental set up is shown schematically in Fig. 1. Particle interaction with the solidification front is studied in a copper chamber with external dimensions 80 mm long, 30 mm wide and 5 mm high, with a machined groove 0.6 mm deep, 5 mm wide and approximately 30 mm long.

In order to establish a suitable temperature gradient along the groove, the chamber may be heated electrically at one end and cooled by circulating water through a copper tube at the other end of the chamber. The temperature of the thermostat water can be increased and decreased by means of a temperature programmer which controls the thermostat.

Coal particles are placed in the groove and covered with powdered matrix material. Then the chamber is covered with a

microscope cover slide. Both the chamber and the cover glass are carefully cleaned before each experiment. The chamber is then mounted on the stage of a microscope. The cell is heated electrically to melt the matrix powder. Once the matrix material has melted, one can control the rate of solidification by controlling the temperature of the heating and cooling units. The velocity of the solidification front can be varied over a wide range by adjusting the temperature programmer.

The interaction between the particle and the solidification front is observed through the microscope using an overall magnification (through the eyepiece) of 64X with reflected light. Particle size was estimated by the use of an eyepiece graticule with squares of suitable dimensions. For more details on the experimental set up see Ref. (14).

Matrix Materials

There are several conditions which the matrix materials must satisfy in order to be used for the engulfing experiments. The matrix material has to be inert, i.e. should not react chemically with the particle materials and must not be toxic. Knowledge of the physical and thermal properties of the matrix materials is also an important criterion for material selection. Furthermore, the matrix materials must form plane solid/liquid interfaces when it solidifies. Dentritic growth leads to immediate entrapment of the particles for steric and not thermodynamic reasons.

At the present time only a limited range of suitable matrix materials is identified but a search for more is continuing.

The physical properties of the matrix materials used for the experiments are summarized in Table 1. All of these materials were used in the level 1 experiments, whereas the critical velocity measurements in level 2 were performed only with thymol, biphenyl and naphthalene.

The matrix materials were Fisher or Eastman products and all of them were zone refined prior to the measurements.

Coal Samples

This study involved three coal samples from Western Canada each consisting of six fraction sizes identified by a mesh range (-60+100, -100+150, -150+200, -200+325, -325+400 and -400 mesh fractions). Two of the coal samples (No. 1 and No. 2) were bitumenous coal, the third sample (No. 3) was a subbitumenous coal. The coal samples were provided by CANMET's Western Research Laboratory, Edmonton, Alta. All coal samples were ground, wet screened and oven dried at 105°C. A coal sample No. 3 which was dry screened after grinding was also studied. The coal samples were stored at room temperature in well closed bottles and they were exposed neither to light nor to heat until use in order to avoid chemical changes of the coal surface.

The dimensional analysis, in level 2, requires the knowledge of a number of physical properties of the particles which are not known precisely, if at all, and which must therefore be determined separately. These quantities are density, ρ_p, specific heat, C_p, and thermal conductivity, k_p, for each fraction size. The density of the coal samples was determined

by means of sample volume measurements using a null pycnometer in the Western Research Laboratory. The specific heat was determined by means of Differential Scanning Calorimetry using a Perkin-Elmer Model DSC-2. More details on these results will be presented in a later paper.

At present there is no suitable technique to measure the actual thermal conductivity of the different coal fractions, but an average thermal conductivity value was estimated as 2.9×10^{-5} [cal/(cm·sec·K)] for coal sample No. 2 (20).

RESULTS AND DISCUSSION

The results of the level 1 experiments are given in Table 2. They show significant differences in the hydrophobicity of the different coal samples.

The low surface tension and the high contact angle values are as expected for bitumenous coals. Coal sample No. 1 has the lowest particle/vapour interfacial tension, γ_{PV}, which corresponds to a contact angle of larger than 82 degrees. This coal sample is the most hydrophobic and therefore would be expected to show the best floatability. The other bitumenous coal, No. 2, has somewhat higher γ_{PV} and lower θ values. The subbitumenous coal No. 3 sample is the least hydrophobic. The engulfing experiments in level 1 show no difference in surface properties between the coal samples No. 3 wet and dry screened, respectively, with the presently available matrix materials. It is apparent that level 1 investigations yield fast information on the approximate surface tensions of coal particles, γ_{PV}, and on the contact angle, θ, with water.

The level 2 investigations were performed with coal samples No. 2 and No. 3 wet and dry screened. Fig. 2 shows a typical plot of solidification front velocity versus particle diameter for the naphthalene/coal No. 2 system. Conventionally, the critical velocity is defined as the velocity which separates rejection and engulfing of particles. All our experiments show, however, that the transition from rejection to engulfing is not sharp, so that we prefer to specify three modes of particle behaviour (14). At relatively high rates of solidification, the particles are engulfed instantly on contact with the solidification front (mode 1). At intermediate rates, the particles are rejected through various distances before being engulfed (mode 2). At relatively low rates of solidification, a steady-state rejection of any individual particle was observed without engulfment (mode 3). The three modes of particle behaviour are represented in Fig. 2 by different symbols. The critical velocity curve is the solid line which was drawn through the data points in such a way that approximately the same number of transition points are above and below it. This choice was modified somewhat by also attempting to have as many open symbols above the curve as solid symbols below. In order to gain information on the actual scatter in the surface tension, γ_{PV}, of the coal particles and their wettability, two broken curves were drawn parallel to the V_c curve at a minimum distance such that these curves were clearly recognizable as unlikely curves representing V_c (15,17). Similar plots are available for biphenyl and thymol (20).

In Fig. 3, the surface tension, γ_{PV}, of coal sample No. 2 and the contact angle with water, θ, are plotted as a function of particle diameter, D, for the naphthalene/coal No. 2 system. The error bars correspond to the width of the transition region of the solidification front velocity-diameter (V-D) curve. The surface tension, γ_{PV}, increases, the contact angle, θ, decreases with increasing particle diameter.

The sensitivity of the method is high, e.g. for naphthalene a 1 erg/cm^2 difference in surface tension or 2 degrees in contact angle correspond to a change in critical velocity of approximately 40 μm/sec. Such large changes are easily observed under the microscope.

The particle engulfment and rejection occurs at the melting temperature of the matrix material so that the surface tension values of the coal samples, determined from different systems, refer to these temperatures. If we want to compare the results obtained from the different systems, the various surface tensions must be referred to the same temperature. From the critical velocity measurements in level 2 we have been able to estimate an average temperature coefficient of particle surface tension as $\frac{d\gamma_{PV}}{dT} = -0.065$ [ergs/(cm^2·K)]. The surface tensions, γ_{PV}, and contact angles with water, θ, were calculated for 20°C by using this average temperature coefficient of surface tension (20).

From level 2 experiments, not discussed here (see Ref. (20)), we estimate a difference of approximately 2 ergs/cm^2 in the

surface tension of coal No. 3 wet and dry screened which could be due to a number of factors, including slime coating; this effect is going to be studied further. The dry screened sample is less hydrophobic. This difference in wettability is supported by ash and moisture content and mineral contamination data. The dry screened subbitumenous coal No. 3 has higher ash and moisture content and is more contaminated with clay minerals, suggesting that wet screening removed inorganic, hydrophilic material.

The second level of analysis is relatively laborious and time consuming. For this reason, we plan to automate these measurements using image analysis and television video techniques. Level 2 investigations can provide a wealth of information on the surface properties of coal particles.

REFERENCES

1. SUN, S. Ch., Transactions AIME 199, 67 (1954).
2. BROWN, D.J., Coal Flotation; D.W. FUERSTENAU: "Froth Flotation" 50th Anniv. Vol., AIME, pp. 51 (1962).
3. HORSLEY, R.M., SMITH, H.G., Fuel 30, 54 (1951).
4. APLAN, F.F., Coal Flotation, in M.C. FUERSTENAU, (ed.): "Flotation", GAUDIN (A.M.) Memorial Flotation Symposium, Rapid City, S.D. Vol. 2, pp. 1235 (1976).
5. BRADY, G.A., GAUGER, A.W., Ind. Eng. Chem. 32, 1599 (1940).
6. NEUMANN, A.W., GOOD, R.J., Techniques of Measuring Contact Angles; GOOD, R.J., STROMBERG, R.R. eds. "Surface and Colloid Science", Vol. 11, Plenum Press, New York, pp. 31-91 (1979).
7. TAGGART, A.F., TAYLOR, T.C. and INCE, C.R., Transactions, AIME 87, 285 (1930).
8. SHEPARD, O.C., Mining and Metallurgy 17, 339 (1936).
9. WARK, I.W., COX, A.B., J. Phys. Chem. 39, 551 (1935).
10. ADAM, N.K., JESSOP, G., J. Chem. Soc. 1925, 1863 (1925).
11. GREEN, E.L., J. Phys. Chem. 33, 921 (1929).
12. WENZEL, R.N., Ind. Chem. Eng. 28, 988 (1936).
13. SPELT, J.K., M.A.Sc. Thesis, University of Toronto, 1980.
14. OMENYI, S.N., NEUMANN, A.W., J. Appl. Phys. 47, 3956 (1976).
15. OMENYI, S.N., NEUMANN, A.W., MARTIN, W.W., LESPINARD, G. and SMITH, R.P., accepted for publication in J. Appl. Phys.
16. SMITH, R.P., M.A.Sc. Thesis, University of Toronto, 1981.
17. OMENYI, S.N., Ph.D. Thesis, University of Toronto, 1978.

18. OMENYI, S.N., SMITH, R.P. and NEUMANN, A.W., J. Colloid Interface Sci. 75, 117 (1980).

19. NEUMANN, A.W., GOOD, R.J., HOPE, C.J. and SEJPAL, M., J. Colloid Interface Sci. 49, 291 (1974).

20. SOULARD, M.R., M.A.Sc. Thesis, University of Toronto, 1980.

LEGEND OF FIGURES

Fig. 1. Sketch of the apparatus.

Fig. 2. Solidification front velocity, V, versus particle diameter, D, for naphthalene – coal sample No. 2.

Fig. 3. Surface tension, γ_{PV}, and contact angle with water, θ, as a function of particle diameter, D, for naphthalene-coal sample No. 2 system.

TABLE 1. THERMAL AND PHYSICAL PROPERTIES OF ORGANIC MATRIX MATERIALS

SUBSTANCE	DENSITY [g/cm^3]	VISCOSITY [Poise]	SPECIFIC HEAT [cal/(g·K)]	THERMAL CONDUCTIVITY [cal/(sec·cm·K)]	SURFACE TENSION γ_{LV}, at melting point [$ergs/cm^2$]
THYMOL	0.925	0.0397	0.566	0.00031	29.9 at 51.5°C
BIPHENYL	0.992	0.0149	0.440	0.00034	32.5 at 70°C
NAPHTHALENE	0.978	0.00967	0.402	0.00054	32.8 at 80°C
SALOL	1.200	0.0889	0.391	0.00020	35.3 at 43°C
2-PHENYL PHENOL	1.210				38.7 at 59°C

TABLE 2. RESULTS AND CONCLUSIONS REGARDING THE "RANKING" SERIES OF ENGULFING EXPERIMENT FOR COAL SAMPLES FROM LEVEL 1 INVESTIGATIONS

COAL SAMPLE (all fraction size)	EXPERIMENTAL OBSERVATION	SURFACE TENSION γ_{PV} [ergs/cm^2]	CONTACT ANGLE OF WATER θ [degrees]
No. 1	Engulfed by all matrix materials	$\gamma_{PV} < 29.9$ at 51.5°C	$\theta > 82.7$ at 51.5°C
No. 2	Rejected by thymol biphenyl naphthalene salol	$\gamma_{PV} > 35.3$ at 43°C	$\theta < 75.3$ at 43°C
	Engulfed by 2-phenyl phenol	$\gamma_{PV} < 38.7$ at 59°C	$\theta > 65.7$ at 59°C
No. 3*	Rejected by all matrix materials	$\gamma_{PV} > 38.7$ at 59°C	$\theta < 65.7$ at 59°C

* Dry as well as wet screened.

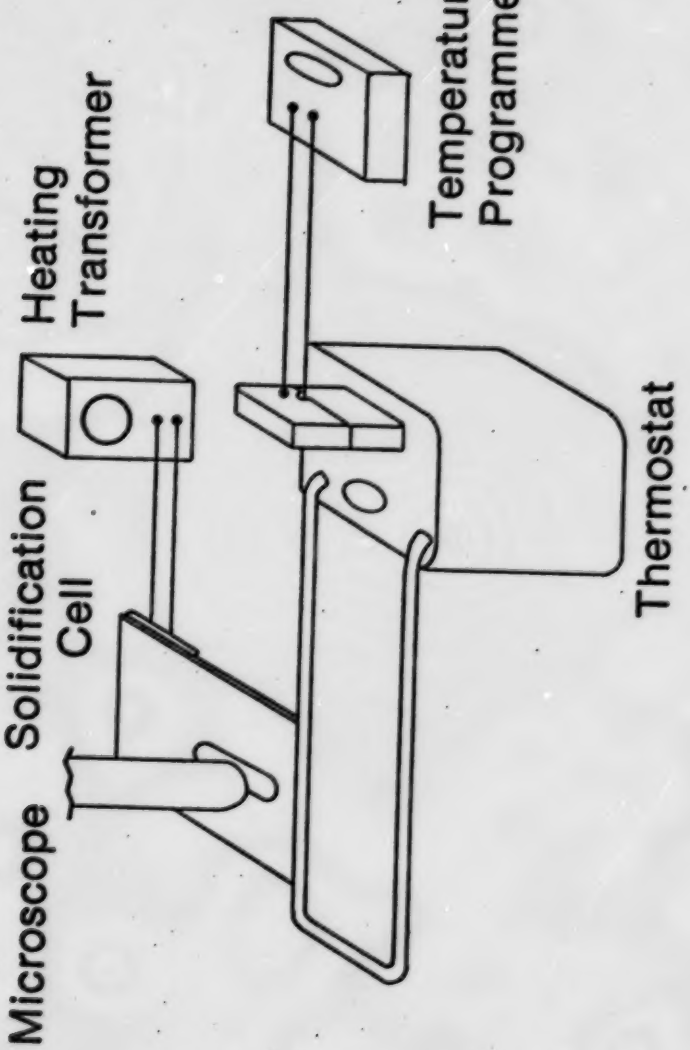
Microscope
Solidification Cell
Heating Transformer
Temperature Programmer
Thermostat

FIGURE 1

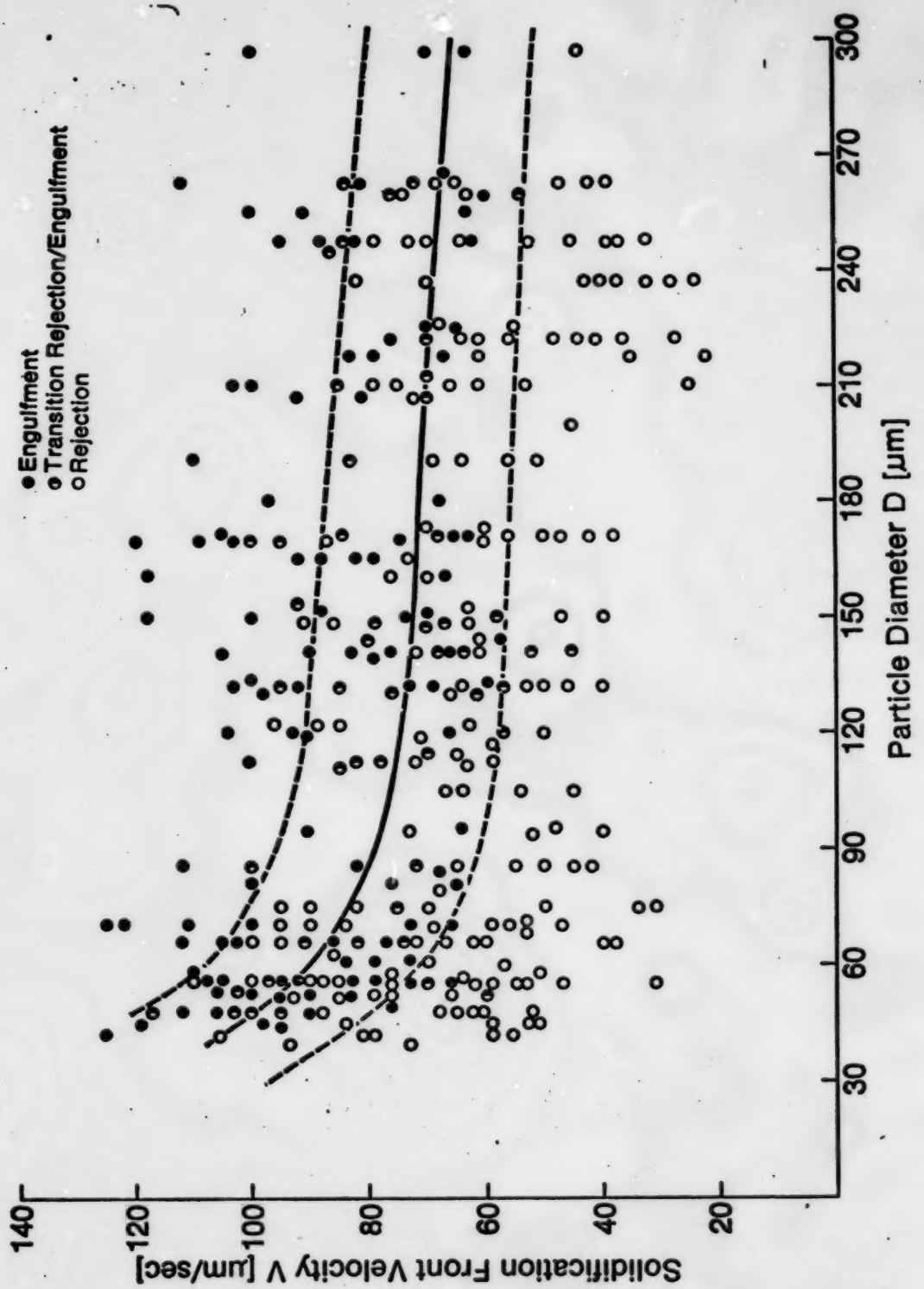
Engulfment
Transition Rejection/Engulfment
Rejection
Solidification Front Velocity V [µm/sec]
140
120
100
80
60
40
20
30
60
90
120
150
180
210
240
270
300
Particle Diameter D [µm]

FIGURE 2

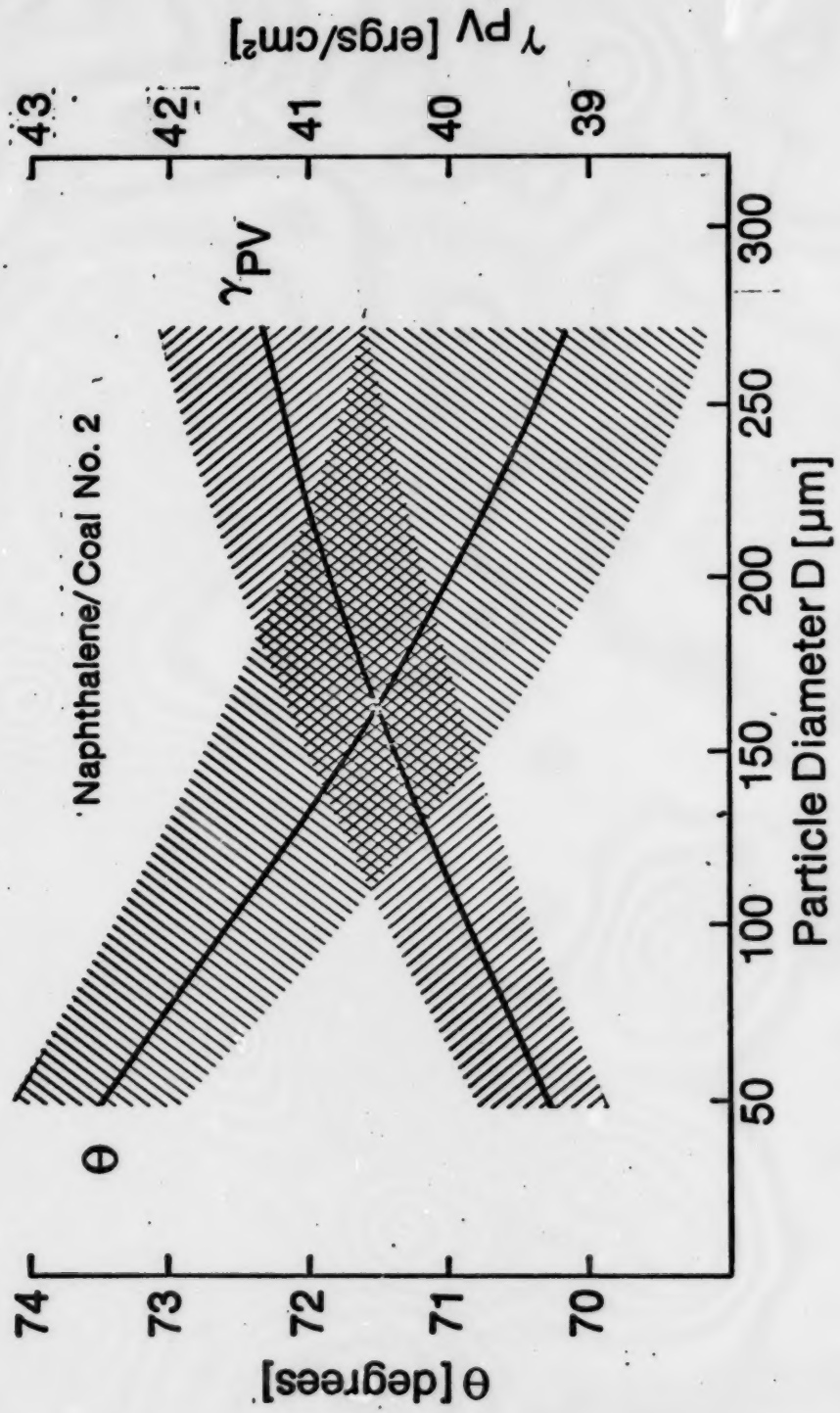
θ [degrees]
74
73
72
71
70
θ
Naphthalene/Coal No. 2
γPV
γ PV [ergs/cm²]
43
42
41
40
39
50
100
150
200
250
300
Particle Diameter D [μm]

FIGURE 3

APPENDIX No.2

WETTABILITY OF COAL PARTICLES: CONTACT ANGLE MEASUREMENTS FROM SOLIDIFICATION FRONT EXPERIMENTS

M.R. Soulard*, E.I. Vargha-Butler*, H. Hamza+ and A.W. Neumann*

*University of Toronto
Department of Mechanical Engineering
5 King's College Road
Toronto, Ontario, Canada

+EMR, Western Research Laboratory CANMET
Edmonton, Alberta, Canada

ABSTRACT

Reliable methods for the characterization of the surface properties and the wettability of coal particles have not been available in the past. The determination of surface tensions and contact angles of coal particles is of great interest in connection with coal beneficiation processes such as froth flotation and oil agglomeration.

A novel technique, based on the behaviour of the test particles at the solidification front of carefully selected, well defined solidifying melts (matrix materials) has been developed recently in our laboratory. This method was used to determine contact angles and surface tensions of coal particles in the range of 20-250 μm. Two types of bituminous and one type of subbituminous coal from Western Canada were tested using thymol, biphenyl, naphthalene, salol and 2-phenyl phenol as matrix materials.

The results show that contact angles on small particles can be determined to within ±2°, i.e. to the same degree of accuracy that is typically reported for extended smooth surface by means of conventional techniques. The measurements also show that within one and the same coal sample the larger particles are somewhat more hydrophilic than the smaller ones.

INTRODUCTION

Escalating prices of energy, which made mining of inferior coal seams more attractive economically, increasing stringency of environmental regulations and mechanization in the coal mining industry contributed in varying degrees to the production of large amounts of fine coal and associated mineral matter especially when dealing with more friable seams such as is the case in Western Canadian coals.

Gravity separation methods for the coal from the mineral matter in this case is technically and/or economically ruled out due to the fineness of the particles under consideration. Therefore one has to exploit differences existing in their surface or interfacial characteristics. Selective surface dependent processes such as flotation and oil agglomeration are being used to varying extents in this regard. These processes mainly rely on exploiting the natural, enhanced or artificially promoted hydrophobicity of the coal particles. This is usually followed in the case of flotation by the introduction of gas bubbles which selectively attach to the hydrophobic component, thus creating solid/gas aggregates of lighter density which levitate to the surface. In the case of oil agglomeration a liquid hydrocarbon is mixed with the suspension to cover selectively the hydrophobic particles which, upon collision, form aggregates with the voids being filled with the liquid hydrocarbon; the mineral matter stays dispersed. The separation of the concentrate from the bulk is achieved in the first case by skimming the floated froth and in the second case by screening out the larger size agglomerates.

Contact angles in the above systems between the gas phase or the liquid hydrocarbon phase and the particle surfaces have been considered for a long time as a useful tool in predicting the behaviour of a given component of the solid system and shows whether it will report to the concentrate or the tailings. This information is valuable for the prediction of yields and grades of various products and hence in the design, operation and control of coal preparation plants.

A mathematical analysis[1,2,3] shows that for spherical and cylindrical particles and densities of the three phases comparable with those in coal-water-air systems flotation is possible for contact angles as low as 50° or 60°, in qualitative agreement with the empirical limiting value for coal of 60-65°[4,5].

Many physical properties influence the wettability of coal. The rank (carbon content) of the coal is a good indication of floatability, most likely because it approximately correlates with the elemental composition[6]. Generally, the contact angle and flotation vary in a regular fashion with the dry mineral matter and free carbon content of the coal[6]. There are indications that floatability is proportional to the surface area (related to porosity) and inversely proportional to particle mass[6]. The order of floatability may change as the amount of mineral matter or ash content associated with the coal types changes. There is a reduction in the native floatability of coal as the ash content increases. It is the coal with the lowest ash content which floats first. The variation of contact angle with carbon content of coal shows a minimum at approximately

87-88% carbon in the coal (dry mineral matter-free basis)[5]. From these results, it appears that the hydrophobicity increases in the following order:

Peat < lignite < subbituminous coal < bituminous coal < anthracite.

The earlier contact angle measurements were performed with bulk coal samples by means of a sessile drop method[7] or the tilting plate method[8,9] but serious difficulties were encountered in obtaining test specimens of the necessary shape and dimensions. Other methods of contact angle measurements were introduced, such as the captive bubble method[4,7,10,11,12] or contact angle measurement on compressed coal powder after polishing the surface of the tablets of coal. This method is prone to a number of drawbacks mainly due to the fact that the final polished surfaces used for the measurement in many cases bear a remote relation only to the particles involved in real cases partly because polishing removes surface layers and partly because of contamination with polishing powder and other contaminants.

In view of these difficulties, we propose to employ a recently developed novel technique for the measurement of contact angles on small, irregularly shaped particles[13-16]. In essence, the technique consists in a quantitative study of the interaction of individual particles initially suspended in the melt of a suitably chosen material, with the solidification front.

2. PARTICLE ENGULFING STUDIES

This method considers the behaviour of the test particles typically in the range of 20-250 μm at the solidification front

of solidifying matrix materials such as pinacol, thymol, biphenyl, naphthalene, salol and 2-phenyl phenol. Particles may either be pushed along by the solidification front or may be engulfed. There are six interfacial tensions which play a role in engulfing and rejection, either directly or indirectly. Three of these are primary, independent single material properties:

γ_{SV}: interfacial tension between the solid matrix material and the vapour phase;

γ_{LV}: interfacial tension between the liquid matrix material and the vapour phase;

γ_{PV}: interfacial tension between the particle and the vapour phase.

As the particles, the solid and liquid matrix materials all form interfaces with each other, the corresponding interfacial tensions must also be considered. They are:

γ_{SL}: interfacial tension between solid and liquid melt;

γ_{PL}: interfacial tension between particle and liquid matrix;

γ_{PS}: interfacial tension between particle and solid matrix.

The three interfacial tensions γ_{SL}, γ_{PS} and γ_{PL} are not independent of the three primary interfacial tensions γ_{SV}, γ_{LV}, γ_{PV}; they are interrelated through equation of state type of relations[19]:

$$\gamma_{SL} = \frac{[(\gamma_{SV})^{\frac{1}{2}} - (\gamma_{LV})^{\frac{1}{2}}]^2}{1 - 0.015(\gamma_{SV}\gamma_{LV})^{\frac{1}{2}}} \qquad (1)$$

$$\gamma_{PL} = \frac{[(\gamma_{PV})^{\frac{1}{2}} - (\gamma_{LV})^{\frac{1}{2}}]^2}{1 - 0.015(\gamma_{PV}\gamma_{LV})^{\frac{1}{2}}} \qquad (2)$$

$$\gamma_{PS} = \frac{[(\gamma_{PV})^{\frac{1}{2}} - (\gamma_{SV})^{\frac{1}{2}}]^2}{1 - 0.015(\gamma_{PV}\gamma_{SV})^{\frac{1}{2}}} \qquad (3)$$

Our approach has two levels.

2.1 Level 1 Approach

The first level in this investigation consists of the "ranking" of the coal samples in comparison with the liquid-vapour interfacial tension, γ_{LV}, of the organic matrix materials. At low solidification rates, the liquid and the solid phases may be assumed to be in thermodynamic equilibrium, so that particle engulfment or rejection is predicted by the net change in free energy, ΔF_{net}, of the particle at the interface:

$$\Delta F_{net} = \gamma_{PS} - \gamma_{PL} \qquad (4)$$

If this overall change in free energy for the process is negative, then particle engulfment is favoured; and if it is positive, then particle rejection by the advancing solid-liquid interface is predicted. Two cases are possible[21]:

Case 1

Given $\gamma_{SV} < \gamma_{LV}$ then

- if $\gamma_{PV} < \gamma_{LV}$, particle engulfment is predicted;
- if $\gamma_{PV} > \gamma_{LV}$, particle rejection is favoured.

All of the matrix materials considered here belong to this category.

Case 2

Given $\gamma_{SV} > \gamma_{LV}$ then

- if $\gamma_{PV} < \gamma_{SV}$, particle rejection is favoured;
- if $\gamma_{PV} > \gamma_{SV}$, particle engulfment is predicted.

An ice-water system is an example of this category.

Therefore it is possible to determine a range in which the surface tension of the coal particles falls by performing a

series of engulfing experiments with matrices of different surface tension, γ_{LV}. For a given matrix material, the particle-solidification front interaction is observed at very low rates of solidification. The particle is either pushed by the solidification front or engulfed. Experiments with different matrix materials determine a lower and upper limit for the range of γ_{PV}. The corresponding contact angle range is calculated by means of an equation-of-state type relation[19]. Although several matrix materials are required, the measurements are relatively easily and quickly performed. Plates 1 to 4 show coal particles being rejected at the solidification front of thymol. Plates 5 to 8 show the particle size dependence of particle rejection at the solidification front of thymol. As the solidification rate increases, the larger particles will be engulfed before the smaller ones. These photomicrographs of particle rejection/engulfment at a solidification front demonstrate the basic simplicity of the freezing front experiment.

2.2 Level 2 Approach

The second level of the investigation involves the determination of the critical velocity of engulfment, V_c. The driving forces for particle rejection are provided by the interfacial free energies whereas the main retarding force is hydrodynamic drag. As the rate of solidification increases the viscous drag opposing the particle motion will increase and at a certain rate, called critical velocity, V_c, the two forces become equal and engulfing occurs. The various particle and matrix (melt) properties that appear in the expressions for the driving and

retarding forces can be related by the method of dimensional analysis. V_c can be determined experimentally and correlated with the free energy of adhesion

$$\Delta F^{adh} = \gamma_{PS} - \gamma_{PL} - \gamma_{SL} \tag{5}$$

In a previous paper[14], a dimensional analysis of this process was formulated, leading to the following relation between non-dimensional groups

$$Re = h\hat{F}^{\ell}\, Q^{m}\, Le^{n} \tag{6}$$

In Eq. (6)

$$Re = \frac{\rho_L V_c D}{\mu}$$

is the Reynolds number,

$$F = \frac{\Delta F^{adh}}{\rho_P C_p DT}$$

is the ratio of free energy of adhesion to the heat capacity

$$Q = \frac{\Delta F^{adh}}{(\mu k_p T)^{\frac{1}{2}}}$$

and

$$Le = \frac{D_L}{\alpha_L}$$

is the Lewis number of the melt. In the above relations, the various symbols represent:

V_c = critical velocity of engulfment [m/sec];

D = diameter of particle [m];

ΔF^{adh} = free energy of adhesion [mJ/m^2];

ρ_L = density of matrix material [kg/m^3];

ρ_P = density of particle [kg/m^3];

μ = viscosity of matrix material [$N \cdot s/m^2$];

C_P = specific heat of particle [$J/kg \cdot K$];

T = melting point of matrix (K);

k_P = thermal conductivity of particle [$J/(m \cdot s \cdot K)$];

D_L = self-diffusion coefficient of the liquid phase;

α_L = thermal diffusivity of the melt defined by $\alpha_L = \frac{k_L}{\rho_L C_L}$;

where

k_L = thermal conductivity of the melt [$J/(m \cdot s \cdot K)$];

C_L = specific heat of the melt [$J/kg \cdot K$].

Values of the constants h, ℓ, m and n in Eq. (2) were determined by multi-variable regression[17]. Re-arranging Eq. (2) the following expression is obtained:

$$\Delta F^{adh} = 6070 \; \frac{\rho_L^{0.6854} \; T^{0.3995}}{\mu^{0.0849}} \; \frac{k_P^{0.6005}}{(\rho_P C_P)^{0.2009}} \; D^{0.4844} \; V_c^{0.6854} \qquad (7)$$

The thermal and physical properties of the organic matrix materials are given in Table 1. With these data, it is possible to obtain ΔF^{adh} from experimental V_c data, using Eq. (7). It is our goal to determine surface properties of the coal particles, i.e. we wish to determine γ_{PV}. As we are working with matrix materials which were characterized previously[16], γ_{SV} and γ_{LV} and hence γ_{SL} through Eq. (1) are known. The free energy of adhesion, Eq. (5) therefore contains two unknowns, γ_{PS} and γ_{PL}. The three equations (5), (2) and (3) constitute three equations in the

three unknowns γ_{PS}, γ_{PL} and γ_{PV}, which can therefore be calculated. Knowing now γ_{PV}, the contact angle which any liquid, such as water, with a surface tension γ_{L*V} would make on a material with the surface tension γ_{PV} may be calculated as follows: First, one calculates γ_{PL*} from

$$\gamma_{PL*} = \frac{[(\gamma_{PV})^{\frac{1}{2}} - (\gamma_{L*V})^{\frac{1}{2}}]^2}{1 - 0.015(\gamma_{PV}\gamma_{L*V})^{\frac{1}{2}}} \tag{8}$$

and then from Young's equation

$$\gamma_{PV} - \gamma_{PL*} = \gamma_{L*V} \cos \theta \tag{9}$$

the contact angle θ for the liquid in question.

The above calculations are performed in this way in principle only. In reality, due to mathematical limitations of Eqs. (1-3) and (8) more general computer programs are used[19,22].

2.3 Experimental Apparatus

The experimental apparatus is shown schematically in Fig. 1. The particle interaction with the solidification front is studied in a cell consisting of a copper block (80 mm x 30 mm x 5 mm) with a machined groove (30 mm x 5 mm x 0.6 mm) in the direction of the largest dimension.

In order to establish a temperature gradient along the groove, the cell is heated electrically at one end while the other end is cooled by water circulating through an attached copper tube. The temperature of the thermostat water can be increased or decreased by means of a temperature programmer.

Coal particles are placed in the groove and covered with powdered matrix material. Then the cell is covered with a

microscope slide. Both the copper cell and the cover glass are cleaned carefully before each experiment. The cell is mounted on the stage of a microscope. Once the matrix material has melted, solidification is initiated and regulated by controlling the temperature of the heating and cooling units. The velocity of the solidification front can be changed over a wide range by adjusting the temperature programmer.

The solidification front-particle interaction may be observed through the microscope with reflected light. Particle size is estimated by means of an eyepiece graticule. For more details on the experimental set-up see Ref. 20 and 21.

3. EXPERIMENTAL RESULTS

This study involved three coal samples from Western Canada provided by CANMET, Western Research Laboratories, Edmonton, Alberta. Two of the coal samples (No. 1 and No. 2) were bituminous and the third sample (No. 3) was a subbituminous coal. Each sample consisted of six size fractions identified by a mesh range (-60+100, -100+150, -150+200, -200+325, -325+400 and -400 mesh fractions). Coal samples No. 1, No. 2 and No. 3 were wet screened and oven dried at 105°C before the experiments at CANMET, Western Research Laboratories. Also, included were seven dry screened fractions of coal sample No. 3. The coal samples were stored at room temperature in well sealed bottles and were not exposed to light or heat until the experiment in order to minimize possible chemical changes.

3.1 Level 1 Results

As explained earlier, this stage involves the "ranking" or "screening" of the three coal samples in reference to the surface

tension, γ_{LV}, of the organic matrix materials. The relevant physical and thermal properties of the matrix materials used are listed in Table 1.

Even at very low rates of solidification, all fraction sizes of coal sample No. 1 were engulfed by thymol, biphenyl, naphthalene, salol and 2-phenyl phenol, indicating low surface tension and high contact angle of this bituminous coal. All fraction sizes of coal No. 2 were pushed by thymol, biphenyl, naphthalene and salol but were engulfed by 2-phenyl phenol.

The freezing front experiments for coal sample No. 3 (wet and dry screened) showed that all fraction sizes were pushed by thymol, biphenyl, naphthalene, salol and 2-phenyl phenol, indicating that this subbitumenous coal is more hydrophilic than both bituminous coals. The implications for the surface tension γ_{PV} and the contact angle θ for water are summarized in Table 2 for all three coal samples.

3.2 Level 2 Results

The second level of the investigation involved the determination of the critical velocity of engulfing V_c as a function of particle diameter for the matrix materials thymol, biphenyl and naphthalene[21].

For coal sample No. 2, the plots of the rate of freezing, V, versus particle diameter, D, for thymol, biphenyl and naphthalene are shown in Figs. 2, 3 and 4, respectively. There are three modes of particle interaction, distinguished by different symbols and referred to as "rejection", "engulfment" and "transition rejection/engulfment". The identification of these three modes

reflects the fact that the transition from "rejection" to "engulfing" is not sharp. There are instances where the particle, when encountered by the solidification front, is reoriented and possibly transported through a short distance before being engulfed.

The critical velocity curve is the solid line which was drawn through the data points in such a way that approximately the same number of transition points (mode 2, half-open symbols) are above and below it. This choice was modified somewhat by also attempting to have as many open symbols above the curve as solid symbols below. In order to gain information on the actual scatter in the surface tension, γ_{LV}, of the coal particles and their wettability, two broken curves were drawn parallel to the V_c curve at a minimum distance such that these curves were clearly recognizable as unlikely curves representing the critical velocity, V_c. Although this procedure will be replaced by a more definite statistical procedure at a later stage, it is apparent that its implementation is not urgent as far as practical considerations are concerned. Comparing, e.g. the solidification front velocity data of Fig. 4 with the corresponding contact angles θ of Fig. 9, it is clear that the band width of Fig. 4 corresponds to an uncertainty in the contact angle of only $\pm 2°$. This is also the error limit typically quoted in contact angle measurements with large, smooth solid surfaces by conventional techniques. These matters were discussed more fully elsewhere[14,15].

For coal sample No. 3 (wet and dry screened) freezing front experiments with thymol using all fraction sizes and with biphenyl

using only fractions -100+150 and -325+400 mesh were performed. The plots of freezing front velocity, V, versus particle diameter, D, for thymol and biphenyl are shown in Figs. 5, 6, 7 and 8. The higher hydrophilicity of the dry screened sample relative to the wet screened sample is apparent in the plots. (See Figs. 5 and 6 for thymol and Figs. 7 and 8 for biphenyl).

Eq. (3) contains physical properties of the particles which must be determined separately. These quantities are density, ρ_P, specific heat, C_P, and thermal conductivity, k_P, for each fraction size. The density of the three coal samples was determined by means of sample volume measurements using a null pycnometer. Table 3 summarizes the density values for the three coal samples. The specific heat of each fraction size for the three coal samples was determined by means of differential scanning calorimetry using a Perkin-Elmer Model DSC-2. Table 4 summarizes the results for coal sample No. 2. More details will be given elsewhere.

The final property required to determine ΔF^{adh} from V_c is the thermal conductivity of the particles. Unfortunately, there is no readily available technique for the determination of the thermal conductivity of small particles.

Therefore, estimates will have to be used here. Particle engulfment and rejection occurs at the melting temperature of the matrix material so that the surface tensions of the coal samples, determined from different systems, refer to those temperatures. If we want to compare the results obtained from the different systems, the surface tensions, γ_{PV}, must be referred

to a standard reference temperature, e.g. to 20°C. This requirement is equivalent to the knowledge of the temperature dependence of the surface tension γ_{PV}. On the other hand, we have available, in Figs. 2-4, three independent measurements, which should, in principle, all have to lead to the same value of γ_{PV} for coal No. 2. However, the results of Tables 3 and 4 indicate that the physical properties of the coal samples, for whatever reason, may change somewhat with particle size. Neglecting this variation, we found by trial and error constant values for k_p and $\frac{d\gamma_{PV}}{dT}$ which provide an acceptable agreement between the results for the runs with the different matrix materials. The guidelines for this empirical search were provided by the γ_{PV} values of the level 1 investigation[21].

For coal sample No. 2, the average temperature coefficient of the surface tension obtained in this fashion is

$$\frac{d\gamma_{PV}}{dT} = - 0.065[mJ/(m^2 \cdot K)]$$

and the value obtained for the thermal conductivity is

$$k_p = 1.214 \times 10^{-2}[J/(m \cdot s \cdot K)]$$

The value obtained for the temperature coefficient of the surface tension is well within the range of more directly measured values of polymeric materials[13]. In view of this fact, the above k_p value may also be reasonable, although it is significantly smaller than typical k_p values for bulk coal.

All the parameters in Eq. 3 are now known. The free energy of adhesion ΔF^{adh} was then calculated for the various particle

sizes from the experimental V_c data from Eq. (3). Surface tensions, γ_{PV}, and contact angles, θ, were calculated using Eqs. 4, 5, 6 and 8. As an illustration, the particle surface tension γ_{PV} and the contact angle θ with water are given in Fig. 9 as a function of particle diameter D. The shaded error bands reflect the width of the transition band in Fig. 4. While such a dependence has not been observed with homogeneous polymer particles, its occurrence is not surprising in view of the results given in Tables 3 and 4 for densities and specific heats. The γ_{PV} values obtained from all three matrix materials is plotted in Fig. 10 as a function of particle diameter D. The corresponding contact angles of water on coal No. 2 are given in Fig. 11. The agreement between the contact angles obtained from the biphenyl and the naphthalene data is as good as one normally obtains on macroscopic, smooth and flat surfaces by means of conventional techniques, normally quoted to be within $\pm 2°$. The deviation of the thymol results is somewhat larger, particularly for the larger particles. We expect further improvements once the problem of the k_p determination is solved.

For coal No. 3, not sufficient data are available yet for an interpretation analogous to the one given above for coal No. 2. Comparison of Figs. 5 and 6, as well as of Figs. 7 and 8 indicate clearly that the critical velocities of the dry screened particles are higher than those of the wet screened particles. This implies that the wet screened particles are more hydrophobic than the dry screened particles, which in turn suggests that wet screening removed some hydrophilic contaminants.

In conclusion, we have developed two levels of interpreting coal particle behaviour at solidification fronts in terms of wettability. In level 1, the surface tension of the particle is compared with the surface tension of the melt. A relatively simple microscopic observation decides which of the two surface tensions is larger than the other. Choosing a suitable range of matrix materials allows a screening of the various coal samples. In level 2, the critical velocity of engulfing V_c is measured for individual particles. Although the technique is as yet somewhat laborious, it has considerable potential because of its high sensitivity.

ACKNOWLEDGEMENTS

This work was supported by EMR contract No. 20SU.23440-0-9021.

REFERENCES

1. Rapacchietta, A.V., Neumann, A.W. and Omenyi, S.N. J. Colloid Interface Sci., 59, 541 (1977).
2. Rapacchietta, A.V. and Neumann, A.W. J. Colloid Interface Sci., 59, 555 (1977).
3. Neumann, A.W., Economopoulos, O., Boruvka, L. and Rapacchietta, A.V. J. Colloid Interface Sci., 71, 293 (1979).
4. Sun, S.Ch. Trans. AIME, 199, 67 (1954).
5. Brown, D.J. "Coal Flotation", in D.W. Fuerstenau (ed.): "Froth Flotation", 50th Anniv. Vol. AIME (1962).
6. Aplan, F.F. "Coal Flotation", in M.C. Fuerstenau (ed.): "Flotation", Gaudin (A.M.) Memorial Flotation Symposium, Rapid City, S.D., Vol. 2, pp. 1235 (1976).
7. Brady, G.A. and Gauger, A.W. Ind. Eng. Chem., 32, 1599 (1940).
8. Green, E.L. J. Phys. Chem., 33, 921 (1929).
9. Wenzel, R.N. Ind. Chem. Eng., 28, 988 (1936).
10. Horsley, R.M. and Smith, H.G. Fuel, 30, 54 (1951).
11. Shepard, O.C. Mining and Met., 17, 339 (1936).
12. Wark, I.W. and Cox, A.B. J. Phys. Chem., 39, 551 (1935).
13. Omenyi, S.N. Ph.D. Thesis, University of Toronto, 1978.
14. Omenyi, S.N., Neumann, A.W., Martin, W.W., Lespinard, G.M. and Smith, R.P. J. Appl. Phys. (Accepted for publication).
15. Omenyi, S.N., Smith, R.P. and Neumann, A.W. J. Colloid Interface Sci., 75, 117 (1980).
16. Omenyi, S.N., Neumann, A.W. and van Oss, C.J. J. Appl. Phys. (Accepted for publication).
17. Smith, R.P. M.A.Sc. Thesis, University of Toronto, 1981.

18. Ward, C.A. and Neumann, A.W. J. Colloid Interface Sci., 49, 286 (1974).

19. Neumann, A.W., Good, R.J., Hope, C.J. and Sejpal, M. J. Colloid Interface Sci., 49, 291 (1974).

20. Omenyi, S.N. and Neumann, A.W. J. Appl. Phys., 47, 3956 (1976).

21. Soulard, M.R. M.A.Sc. Thesis, University of Toronto, 1980.

22. Neumann, A.W., Hum, O.S. and Francis, D.W. J. Biomed. Mat. Res., 14, 499 (1980).

Legend of Figures

Figure 1 Sketch of the apparatus.

Figure 2 Solidification front velocity, V, versus particle diameter, D, for thymol-coal sample No. 2 wet screened.

Figure 3 Solidification front velocity, V, versus particle diameter, D, for biphenyl-coal sample No. 2 wet screened.

Figure 4 Solidification front velocity, V, versus particle diameter, D, for naphthalene-coal sample No. 2 wet screened.

Figure 5 Solidification front velocity, V, versus particle diameter, D, for thymol-coal sample No. 3 wet screened.

Figure 6 Solidification front velocity, V, versus particle diameter, D, for thymol-coal sample No. 3 dry screened.

Figure 7 Solidification front velocity, V, versus particle diameter, D, for biphenyl-coal sample No. 3 wet screened.

Figure 8 Solidification front velocity, V, versus particle diameter, D, for biphenyl-coal sample No. 3 dry screened.

Figure 9 Particle surface tensions, γ_{PV}, and contact angles, θ, with water versus particle diameter, D, for naphthalene-coal sample No. 2 wet screened.

Figure 10 Particle surface tensions, γ_{PV}, versus particle diameter, D, for the three matrix materials-coal sample No. 2 wet screened.

Figure 11 Contact angles, θ, with water versus particle diameter, D, for the three matrix materials-coal sample No. 2 wet screened.

Legend of Plates

Plates 1-4 Coal particles being rejected at the solidification front of thymol.

Fraction size: 45-74 μm.

Particle diameter: 60 μm.

Front velocity approximately 4 μm/sec.

In each photomicrograph the solidification front is moving diagonally from right to left. The coal particles are rejected by the solidification front.

Plates 5-8 Particle size dependence of particle rejection at the solidification front of thymol.

Fraction size: 45-74 μm.

Particle diameters: Middle particle = 45 μm;
Right particle = 60 μm;
Left particle = 75 μm.

This sequence of photomicrographs shows the rate of solidification increasing from 5 μm/sec to 8 μm/sec. The right particle is pushed slightly and engulfed. The middle particle is pushed and finally is engulfed as the solidification rate increases. The left particle is engulfed immediately. In each photomicrograph the solidification front is moving diagonally from right to left.

TABLE 1. PHYSICAL AND THERMAL PROPERTIES OF THE ORGANIC MATRIX MATERIALS

SUBSTANCE	DENSITY [kg/m³]	VISCOSITY [N·s/m²]	SPECIFIC HEAT [kJ/kg·K]	THERMAL CONDUCTIVITY [J/(m·s·K)]	SURFACE TENSION γ_{SV} AT MELTING POINT [mJ/m²]	SURFACE TENSION γ_{LV} AT MELTING POINT [mJ/m²]
PINACOL	976	*	*	*	28.0 at 43.5°C	28.1 at 43.5°C
THYMOL	925	0.00397	2.370	0.1298	29.4 at 51.5°C	29.9 at 51.5°C
BIPHENYL	992	0.00149	1.842	0.1424	25.6 at 70°C	32.5 at 70°C
NAPHTHALENE	978	0.000967	1.683	0.2261	22.9 at 80°C	32.8 at 80°C
SALOL	1200	0.00889	1.637	0.0837	34.5 at 43°C	35.3 at 43°C
2-PHENYL PHENOL	1210	*	*	*	38.6 at 59°C	38.7 at 59°C

*Information not available.

TABLE 2. RESULTS OF THE LEVEL 1 INVESTIGATION OF THE THREE COAL SAMPLES

Coal Sample (all fractions)	Surface Tension γ_{PV} [mJ/m^2]	Contact Angle of Water θ (degrees)
No. 1	$\gamma_{PV} < 29.9$ at 51.5°C	$\theta > 82.7$ at 51.5°C
No. 2	$\gamma_{PV} > 35.3$ at 43°C	$\theta < 75.3$ at 43°C
	$\gamma_{PV} < 38.7$ at 59°C	$\theta > 65.7$ at 59°C
No. 3 (wet and dry screened)	$\gamma_{PV} > 38.7$ at 59°C	$\theta < 65.7$ at 59°C

TABLE 3. DENSITY VALUES OF COAL SAMPI

FRACTION OF COAL (MESH)	DENSITY [kg/m^3] SAMPLE NO. 1	SAMPLE NO. 2
-60+100	1520	1470
-100+150	1360	1440
-150+200	1320	1410
-200+325	1430	1430
-325+400	1340	1410
-400	1350	1450

TABLE 4. SPECIFIC HEATS FOR COAL SAMPLES NO. 2 WET SCREENED AS RECEIVED

TEMPERATURE	SPECIFIC HEAT C_p[kJ/kg·K] MESH SIZE OF FRACTIONS					
[K]	-60+100	-100+150	-150+200	-200+325	-325+400	-400
300	1.113	1.109	1.033	1.008	1.042	1.050
310	1.134	1.188	1.133	1.100	1.113	1.192
320	1.192	1.259	1.234	1.184	1.230	1.385
330	1.222	1.289	1.314	1.268	1.402	1.418
340	1.218	1.335	1.364	1.322	1.452	1.527
350	1.234	1.305	1.335	1.289	1.418	1.494
360	1.247	1.322	1.351	1.259	1.385	1.460

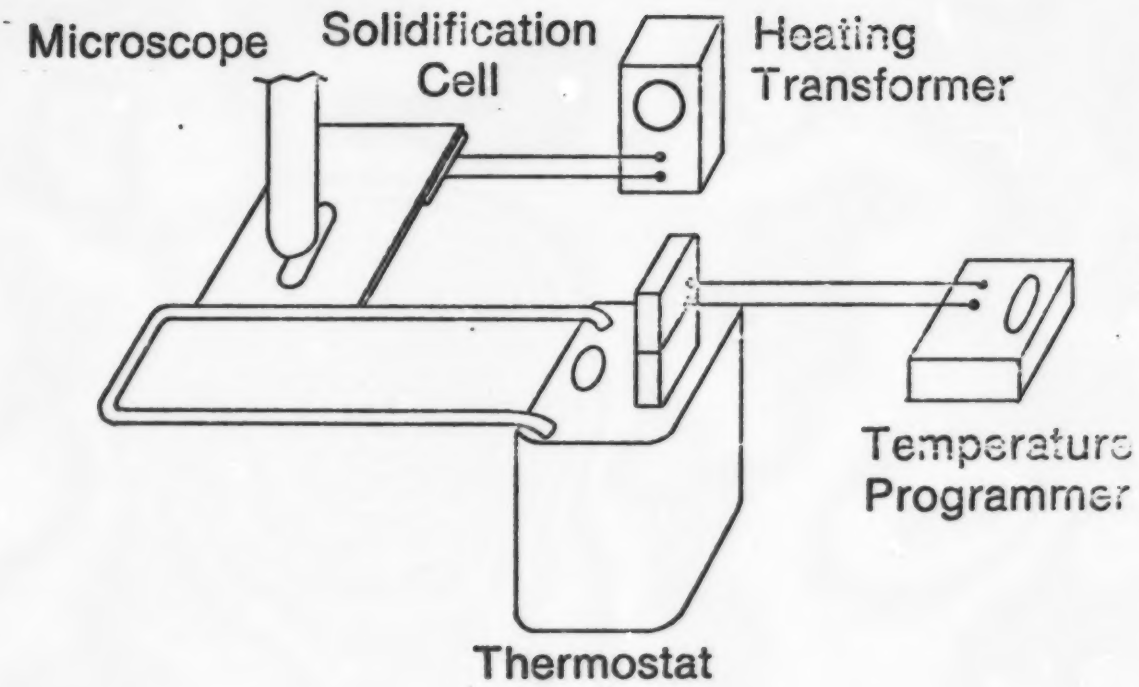
Microscope
Solidification Cell
Heating Transformer
Temperature Programmer
Thermostat

FIGURE 1

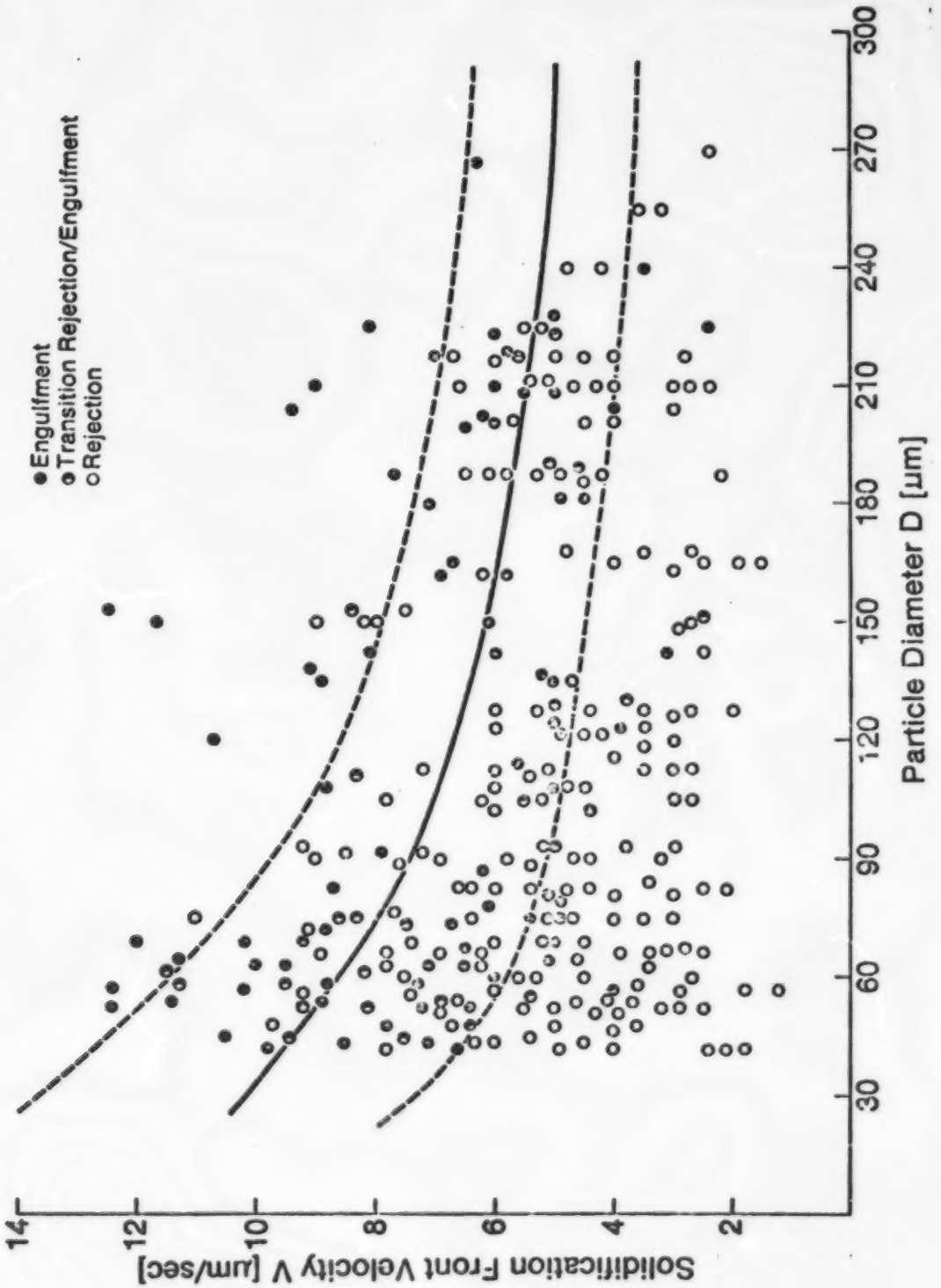
●Engulfment
●Transition Rejection/Engulfment
○Rejection
Solidification Front Velocity V [µm/sec]
14
12
10
8
6
4
2
Particle Diameter D [µm]
30
60
90
120
150
180
210
240
270
300

FIGURE 2

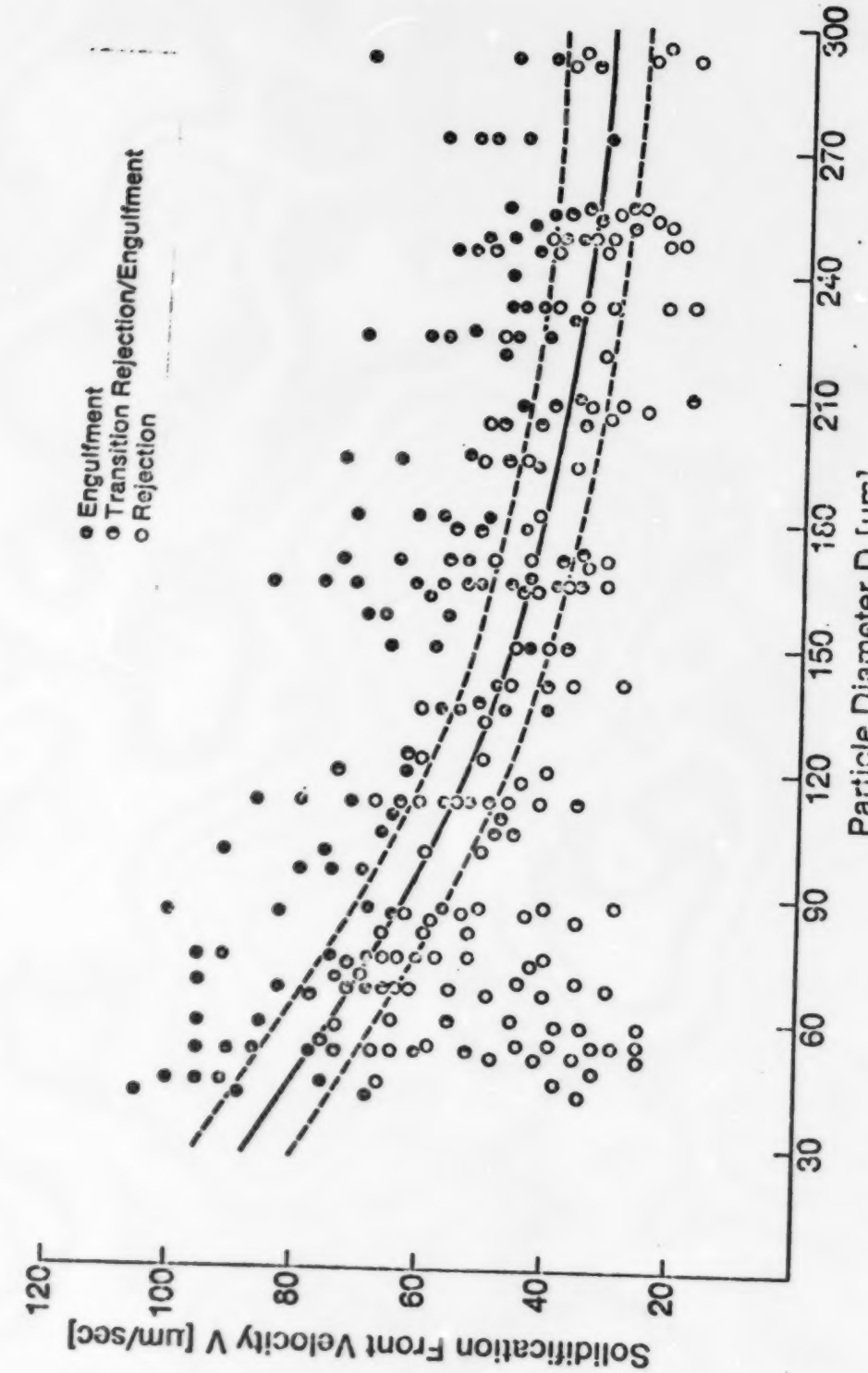
Engulfment
Transition Rejection/Engulfment
Rejection
Solidification Front Velocity V [um/sec]
120
100
80
60
40
20
Particle Diameter D [µm]
30
60
90
120
150
180
210
240
270
300

FIGURE 3

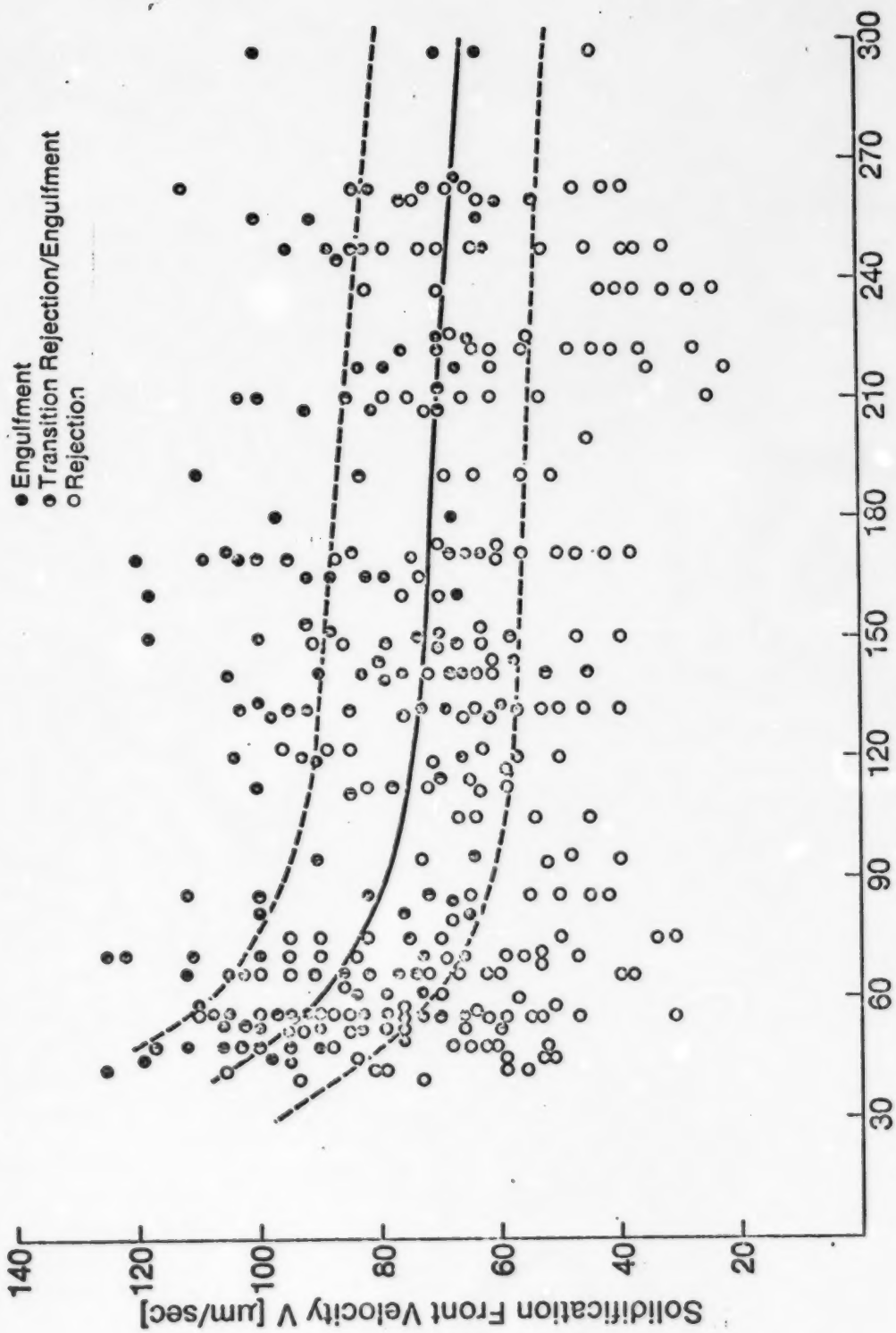
● Engulfment
● Transition Rejection/Engulfment
○ Rejection
Solidification Front Velocity V [µm/sec]
140
120
100
80
60
40
20
30
60
90
120
150
180
210
240
270
300
Particle Diameter D [µm]

FIGURE 4

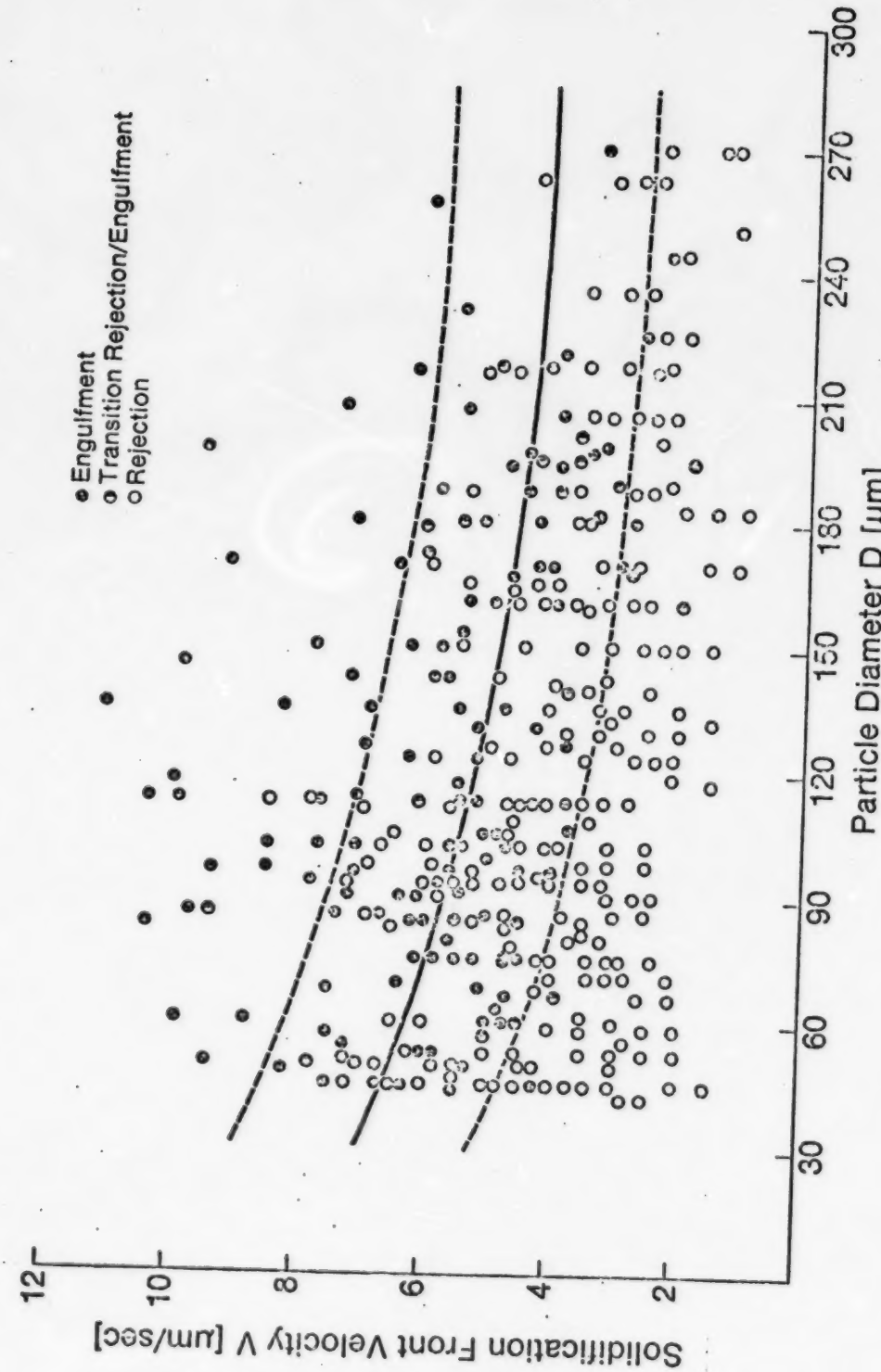
Engulfment
Transition Rejection/Engulfment
Rejection
Solidification Front Velocity V [μm/sec]
12
10
8
6
4
2
30
60
90
120
150
180
210
240
270
300
Particle Diameter D [μm]

FIGURE 5

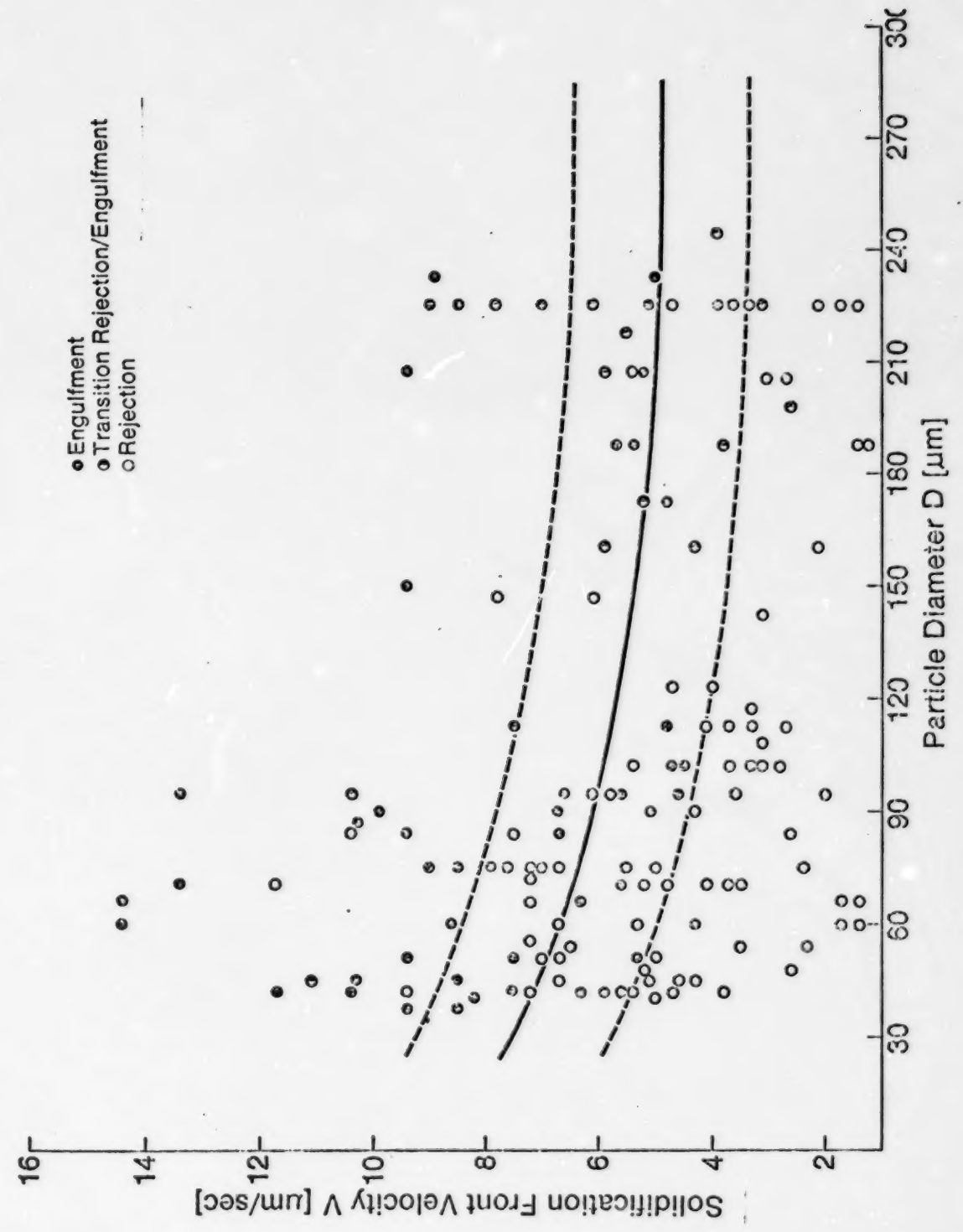
Engulfment
Transition Rejection/Engulfment
Rejection
Solidification Front Velocity V [um/sec]
16
14
12
10
8
6
4
2
30
60
90
120
150
180
210
240
270
Particle Diameter D [µm]

FIGURE 6

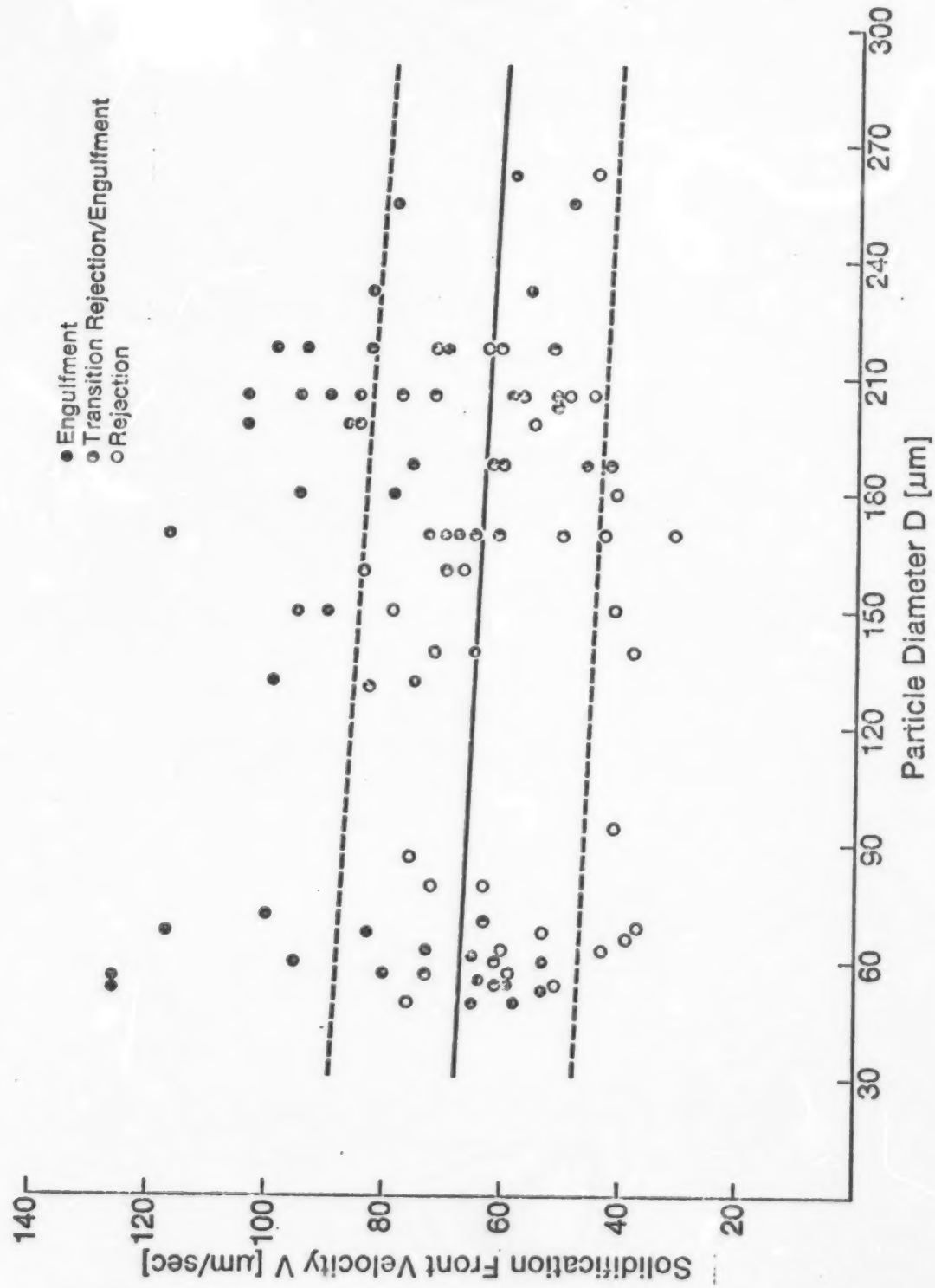
● Engulfment
◍ Transition Rejection/Engulfment
○ Rejection
Solidification Front Velocity V [µm/sec]
140
120
100
80
60
40
20
30
60
90
120
150
160
210
240
270
300
Particle Diameter D [µm]

FIGURE 7

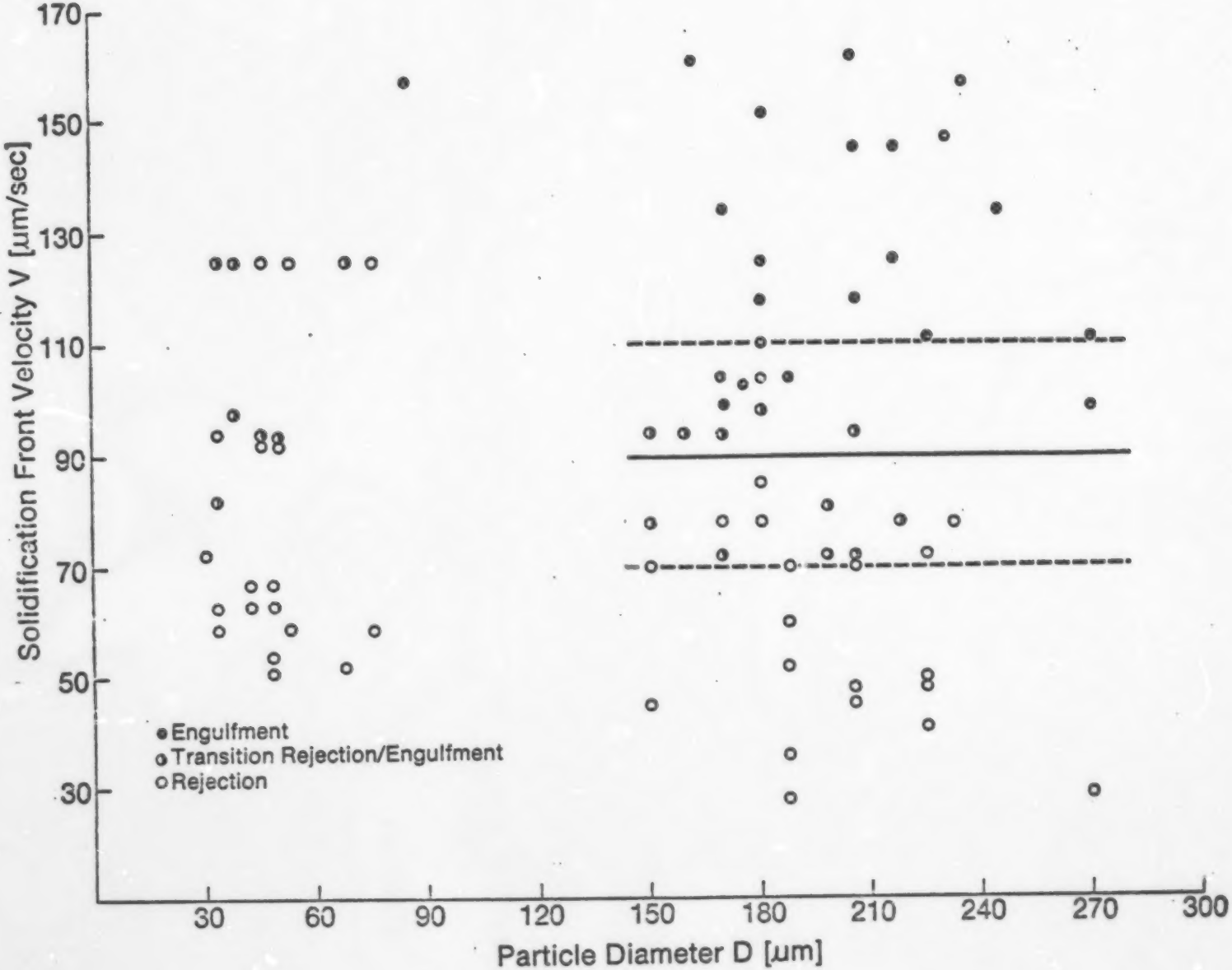
Solidification Front Velocity V [μm/sec]
170
150
130
110
90
70
50
30
Engulfment
Transition Rejection/Engulfment
Rejection
30
60
90
120
150
180
210
240
270
300
Particle Diameter D [μm]

FIGURE 8

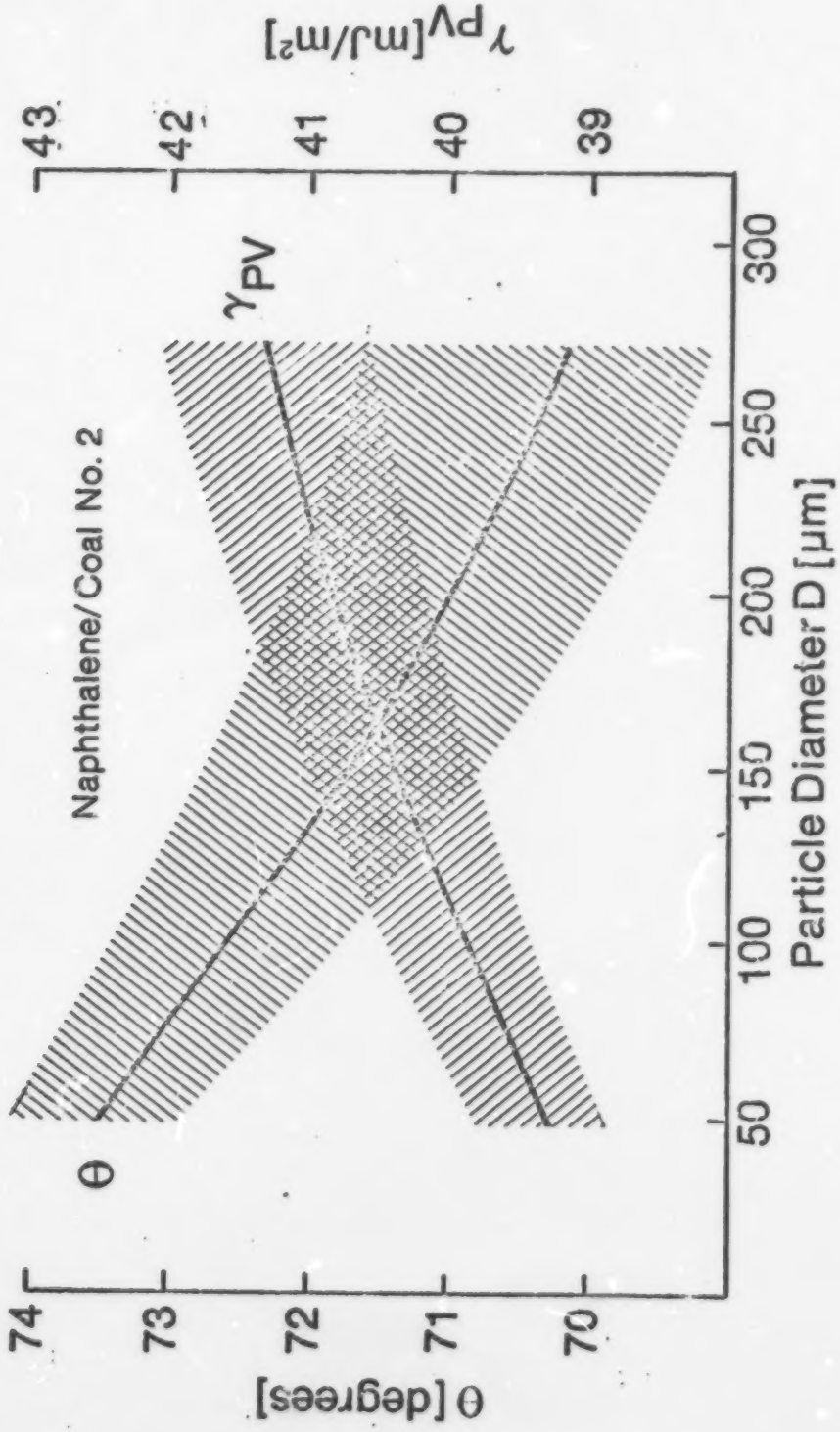
θ [degrees]
74
73
72
71
70
γ_{PV} [mJ/m²]
43
42
41
40
39
Particle Diameter D [μm]
50
100
150
200
250
300
Naphthalene/ Coal No. 2
θ
γ_{PV}

FIGURE 9

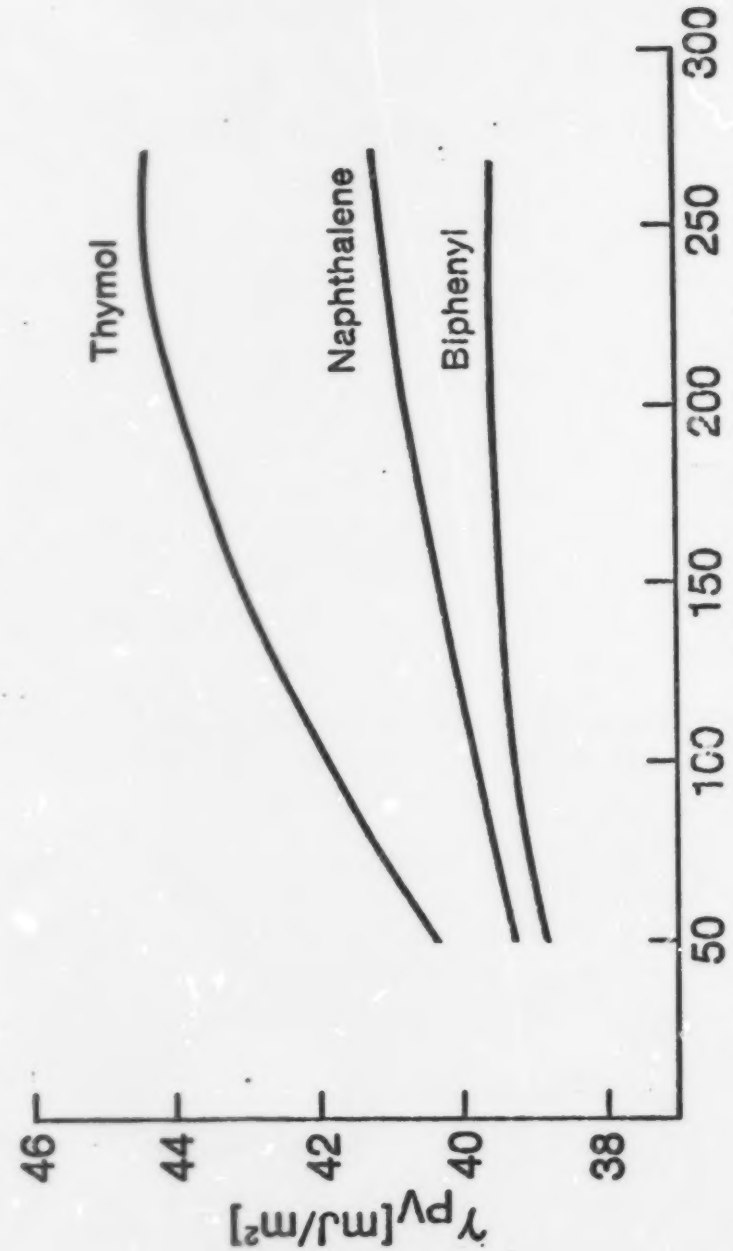
Thymol
Naphthalene
Biphenyl
46
44
42
40
38
50
100
150
200
250
300
Particle Diameter D [µm]
γPV[mJ/m²]

FIGURE 10

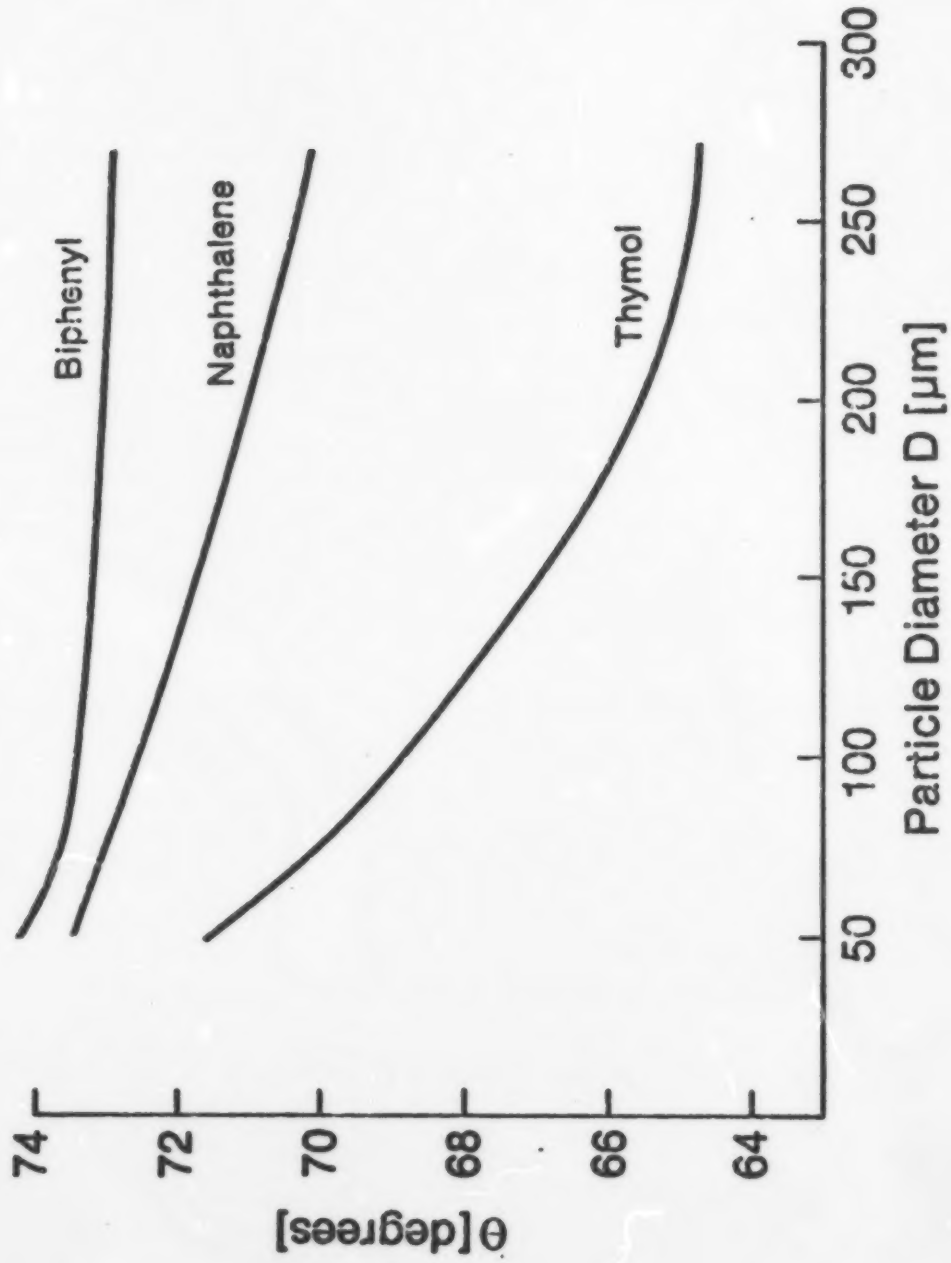
Biphenyl
Naphthalene
Thymol
74
72
70
68
66
64
θ [degrees]
50
100
150
200
250
300
Particle Diameter D [µm]

FIGURE 11

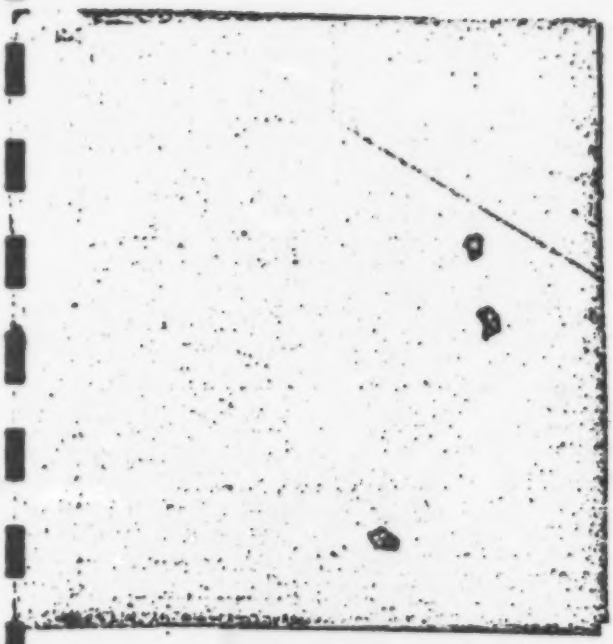

PLATE 1

PLATE 2

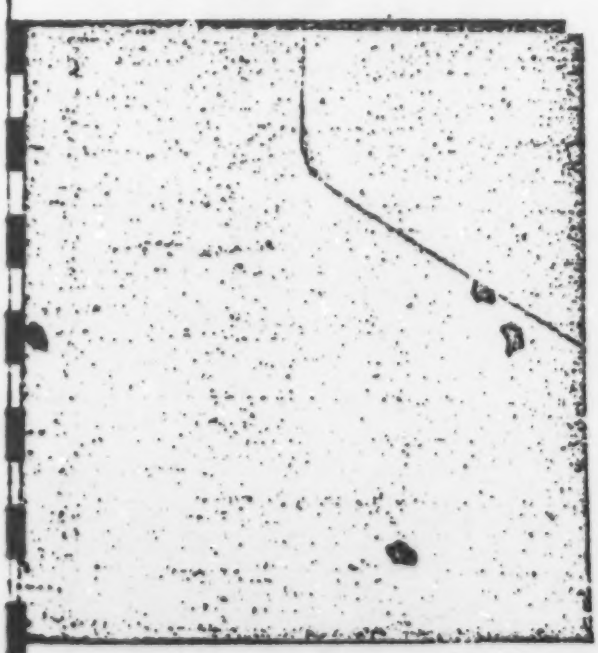

PLATE 3

PLATE 4

PLATE 5

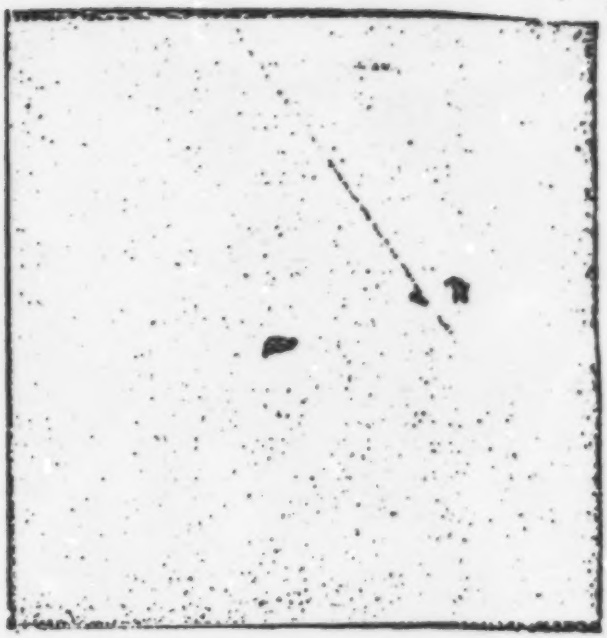

PLATE 6

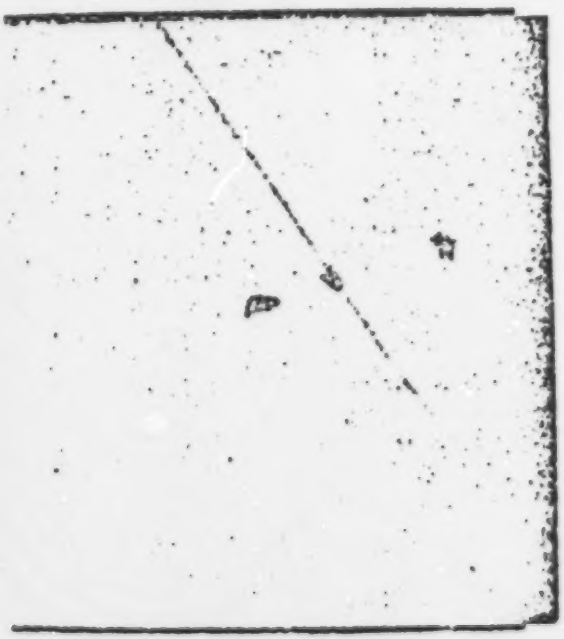

PLATE 7

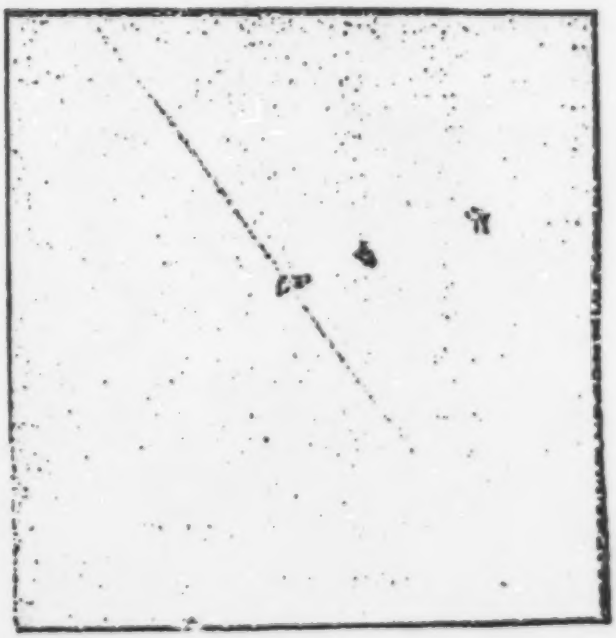

PLATE 8

APPENDIX No.3

TEMPERATURE DEPENDENT SPECIFIC HEATS OF POLYMERS BY DIFFERENTIAL SCANNING CALORIMETRY

E.I. Vargha-Putler[+], H. Hamza* and A.W. Neumann[+]

[+]University of Toronto
Department of Mechanical Engineering
5 King's College Road
Toronto, Ontario Canada

*EMR, Western Research Laboratory
CANMET, Edmonton, Alberta, Canada

INTRODUCTION

Our studies of the specific heat of polymers were motivated by work on the wettability of coal and of other solid particles by means of a freezing front technique.[1-3] Specific heat data are a prerequisite for the quantitative determination of contact angles on solid particles using the above mentioned technique. As such data were not available for coal in powdered form, it was decided to generate them by differential scanning calorimetry (DSC).[4] Since data for comparison were not available, it was also decided to measure the specific heats of several polymeric materials. In order to alleviate a main concern on whether or not DSC specific heat values are dependent on the degree of diminution of the sample (i.e. powder, film, bulk), measurements were performed with several polymers in the form of films, powders and granules. The results appear to be of sufficient interest to be reported here.

EXPERIMENTAL

Materials

The specific heats of the following polymer samples were determined:

1. Poly(propylene), PP, powder (Polysciences Inc.).
2. Poly(styrene), PS, in both powder and film forms with a molecular weight of 20 400 and PS powder with a molecular

weight of 200 000; M_w/M_n less than 1.06 (Pressure Chemical Co., Pittsburgh, Mellon Institute, special PS standard).

3. Poly(hexamethylene adipamide), Nylon 66, PA 66, powder and film (Polysciences Inc.).
4. Poly(tetrafluoroethylene), Teflon, PTFE, granules and powder (Polysciences Inc.).
5. Tetrafluorethylene-hexafluoropropylene copolymer, FEP, film (Commercial Plastics, Toronto).

The polymer films were prepared from the polymer powder either by heat pressing or by means of solvent casting.[5] PTFE and FEP films were prepared by heat pressing, while the films of PP, PS and PA were prepared by solvent casting.

Method

The specific heat measurements were performed in the temperature range from 300 to 360 K using a Perkin-Elmer Model DSC-2 calorimeter. The heating and cooling rate was selected as 10 K/min, the chart range as 5 mV, the range control as 5 mcal/sec and the chart speed as 20 mm/min. These settings were chosen on the recommendation of Perkin-Elmer for C_p measurements. Lower rates give poor sensitivity, higher rates provide greater sensitivity but poorer temperature accuracy. Nitrogen gas of 99.99% minimum purity was used for purging the sample holders. A detailed discussion of the DSC-2 and the specific heat measurements are given in References.[6-8]

An 8.21 mg synthetic sapphire (α- Al_2O_3) standard was used for calibration; the specific heat values of sapphire were obtained from the work of Ginnings and Furukawa.[9] The difference in the weights (ΔW) of the aluminum sample-pans (in which the samples were encapsulated and weighed) were taken into account. The ΔW value defines an additional ordinate displacement (ΔD in mm) which has to be added to the displacement (D in mm) caused by the material in the lighter pan. The ΔW values vary from 0.01 to 2.00 milligrams which, if not corrected, could cause errors in C_p values up to 25%.

The specific heat of the polymer samples, C_p (sample), can be calculated after the calibration with the sapphire disc (ratio method)[8] using the formula

$$C_p \text{ (sample)} = \frac{W \text{ (sapphire)}}{W \text{ (sample)}} \times \frac{D \text{ (sample)}}{D \text{ (sapphire)}} \times C_p \text{ (sapphire)} \qquad (1)$$

where C_p (sapphire) is the specific heat of the sapphire standard in cal/g·K, W (sapphire) and W (sample) are the weights of the standard and of the sample, respectively, in milligrams, D (sapphire) and D (sample) are the corrected ordinate displacements of the sapphire and that of the sample in mm. Finally, the specific heats were expressed in KJ/kg.K.

The specific heat data presented here are the arithmetic mean values of at least three measurements. The standard deviation and the population mean were calculated from the

sample mean assuming a t distribution. The errors given in Table 1 are 95 percent confidence limits.

The samples were reweighed after the experiments but no significant (less than 0.1 mg) change in weight was observed.

RESULTS AND DISCUSSION

In Figures 1 and 2 the specific heats of the various polymer samples are plotted as a function of temperature. For polypropylene, polystyrene and FEP the specific heat increases linearly with temperature over the whole range investigated, as expected.

The slope of the Nylon 66 (PA 66) data changes at about 330 K and of the Teflon (PTFE) data at about 340 K (Fig. 2) suggesting conformational changes. The glass transition temperature, T_g, of Nylon 66 given in the literature[10] shows some scatter, with most values being around 323 K. We feel that the change in slope of the PA 66 plot (Fig. 2) near 330 K is sufficiently close to assume that it is due to the glass transition.

The measurements with PTFE show a change of slope in the specific heat-temperature curve at approx. 340 K, both for the powdered and the granulated (bulk) forms of Teflon (PTFE). No conformational changes for PTFE have been reported in the literature at this temperature until recently, when the second moment of NMR derivative spectra was studied by

Davidson and Gounder[11] on polytetrafluoroethylene specimens deformed to various elongations. The second moments were computed as a function of temperature from 250 to 350 K. A change in second moment was observed at 345 K, which, according to the authors, represented a change in the orientation texture of the crystalline phase. The plot of C_p in Fig. 2 shows a change in slope at approximately 340 K, which might be correlated with such an orientation effect.

As the plots in Figs. 1 and 2 are not adequate for recovering actual data, the results are summarized in Table 1, together with information on the accuracy. A comparison of our results with literature data[10,12] is given in Table 2. The agreement is satisfactory.

CONCLUSIONS

From these measurements no differences were found between the results obtained for powdered and bulk polymers. On the other hand, relatively small differences in chemical structure (PTFE vs. FEP) as well as differences in molecular weight (PS powders with a MW of 20 400 vs 200 000) show considerable differences in the specific heat.

In summary, it appears that differential scanning calorimetry is an appropriate technique for determining the temperature dependence of the specific heat of polymers. The technique

is applicable whether the samples are available in the form of film, powder or granules.

ACKNOWLEDGEMENTS

The work was supported by Energy, Mines and Resources, CANMET, Canada, through contract No. 20SU·23440-0-9021.

References

1. Vargha-Butler, E.I., Soulard, M.R., Hamza, H. and Neumann, A.W. (submitted for publication).

2. Omenyi, S.N., Neumann, A.W. J. Appl. Phys. 47, 3956 (1976).

3. Omenyi, S.N., Smith, R.P. and Neumann, A.W. J. Colloid Interface Sci., 75, 117 (1980).

4. Vargha-Butler, E.I., Soulard, M.R., Hamza, H. and Neumann, A.W. (submitted for publication).

5. Omenyi, S.N. Ph.D. Thesis, University of Toronto, 1978.

6. O'Neill, M.J. Anal. Chem. 36, 1238 (1964).

7. Watson, E.S., O'Neill, M.J. Justin, J. and Brenner, N. Anal. Chem. 36, 1233 (1964).

8. O'Neill, M.J. Anal. Chem. 38, 1331 (1966).

9. Ginnings, D.C., Furukawa, G.T. J. Am. Chem. Soc. 75, 522 (1953).

10. Brandrup, J., Immergut, E.H. Polymer Handbook (2nd Ed.), Wiley, New York, (1975).

11. Davidson, Th., Gounder, R.N. (Editor LEE, L.H.) Adhesion and Adsorption of Polymers, Polymer Science & Technology, Vol. 12B, Plenum, New York (1979), p. 787.

12. van Krevelen, D.V. Properties of Polymers, Elsevier, Amsterdam, (1976) p. 84.

Table 1

TEMPERATURE DEPENDENCE OF SPECIFIC HEATS OF POLYMERS

Temperature	Specific Heat C_p (kJ/kg·K)								
	PP	PS			PA 66		PTFE		FEP
K		MW 20 400	MW 20 400	MW 200 000					
	powder	powder	film	powder	powder	film	powder	granules	film
300	1.680±0.089	1.188±0.077	1.193±0.092	1.185±0.010	1.574±0.079	1.591±0.047	1.098±0.286	1.074±0.042	1.022±0.055
310	1.782±0.152	1.232±0.050	1.239±0.062	1.275±0.067	1.711±0.169	1.722±0.070	1.155±0.102	1.146±0.005	1.046±0.097
320	1.843±0.139	1.285±0.104	1.271±0.057	1.399±0.022	1.824±0.166	1.830±0.065	1.176±0.216	1.190±0.015	1.065±0.094
330	1.978±0.152	1.327±0.109	1.300±0.119	1.445±0.084	1.993±0.147	1.939±0.109	1.239±0.146	1.256±0.010	1.093±0.062
340	2.051±0.099	1.412±0.089	1.401±0.060	1.564±0.005	2.021±0.037	1.991±0.109	1.355±0.089	1.359±0.037	1.104±0.084
350	2.120±0.142	1.481±0.047	1.447±0.070	1.660±0.037	2.054±0.030	2.052±0.147	1.349±0.164	1.358±0.027	1.128±0.025
360	2.159±0.147	1.515±0.032	1.518±0.142	1.698±0.057	2.145±0.052	2.098±0.117	1.362±0.226	1.372±0.032	1.147±0.022

Table 2

COMPARISON OF THE SPECIFIC HEATS

OF POLYMERS WITH LITERATURE DATA

Sample	Specific heat C_P (kJ/kg.K)		
	Literature data	References	Present work
Teflon PTFE	0.960 at 298 K 0.961 at 300 K	12 10	1.086 at 300 K
Poly(styrene) PS	1.220 at 298 K 1.194-1.220 at 298 K 1.256 at 323 K	12 10 10	1.188 at 300 K 1.278 at 320 K
Poly(propylene) PP	1.630-1.760 at 298 K 1.789-1.926 at 298 K	12 10	1.680 at 300 K
Nylon 66 PA 66	1.470 at 298 K 1.419 at 298 K	12 10	1.583 at 300 K

LEGENDS OF FIGURES

Figure 1 Temperature dependence of specific heats of polypropylene and polystyrene

◊ PP powder, o PS powder, MW 20 400, • PS film, MW 20 400, Δ PS powder, MW 200 000.

Figure 2 Temperature dependence of specific heat of PA 66, PTFE and FEP

o PA 66 powder, • PA 66 film, Δ PTFE powder

▲ PTFE granules, ◊ FEP film.

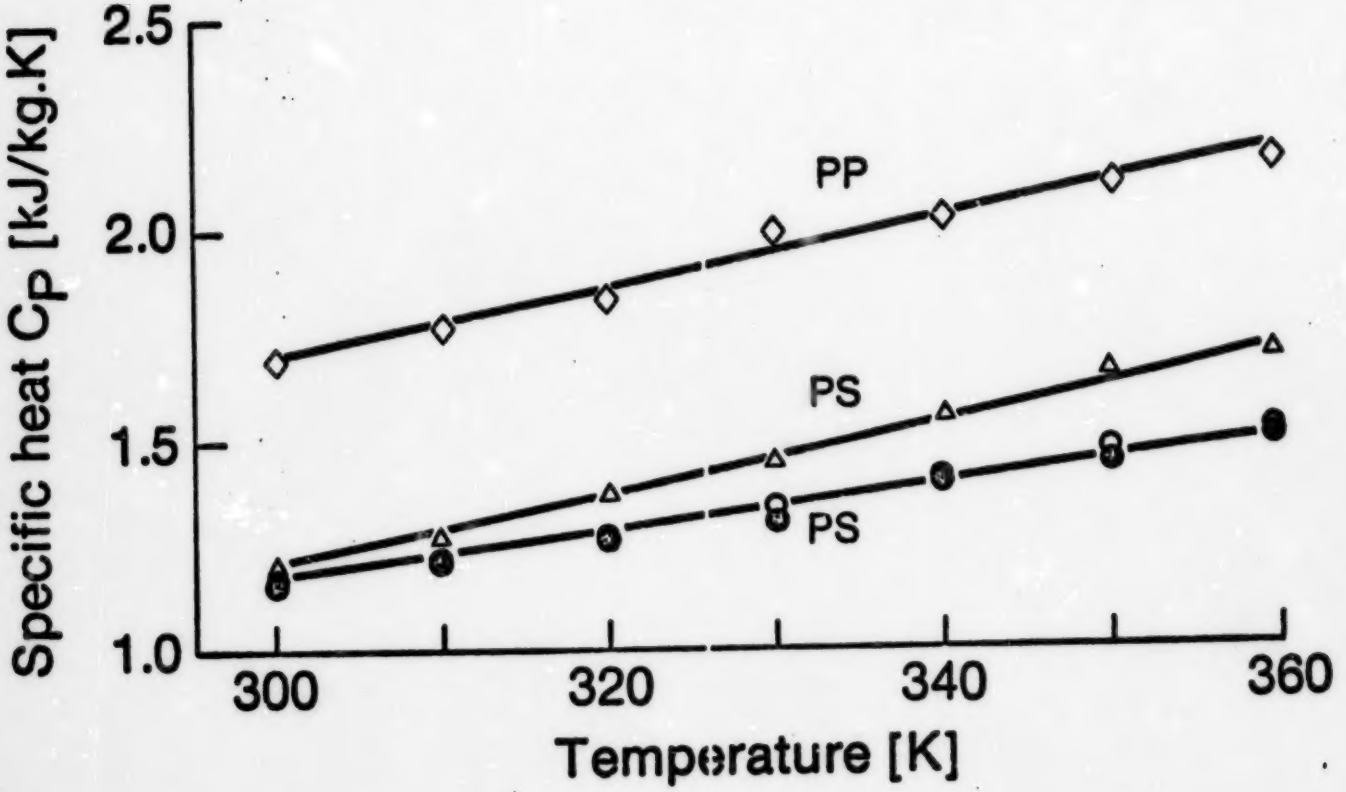
Specific heat C_P [kJ/kg.K]
2.5
2.0
1.5
1.0
300
320
340
360
Temperature [K]
PP
PS
PS

Figure 1

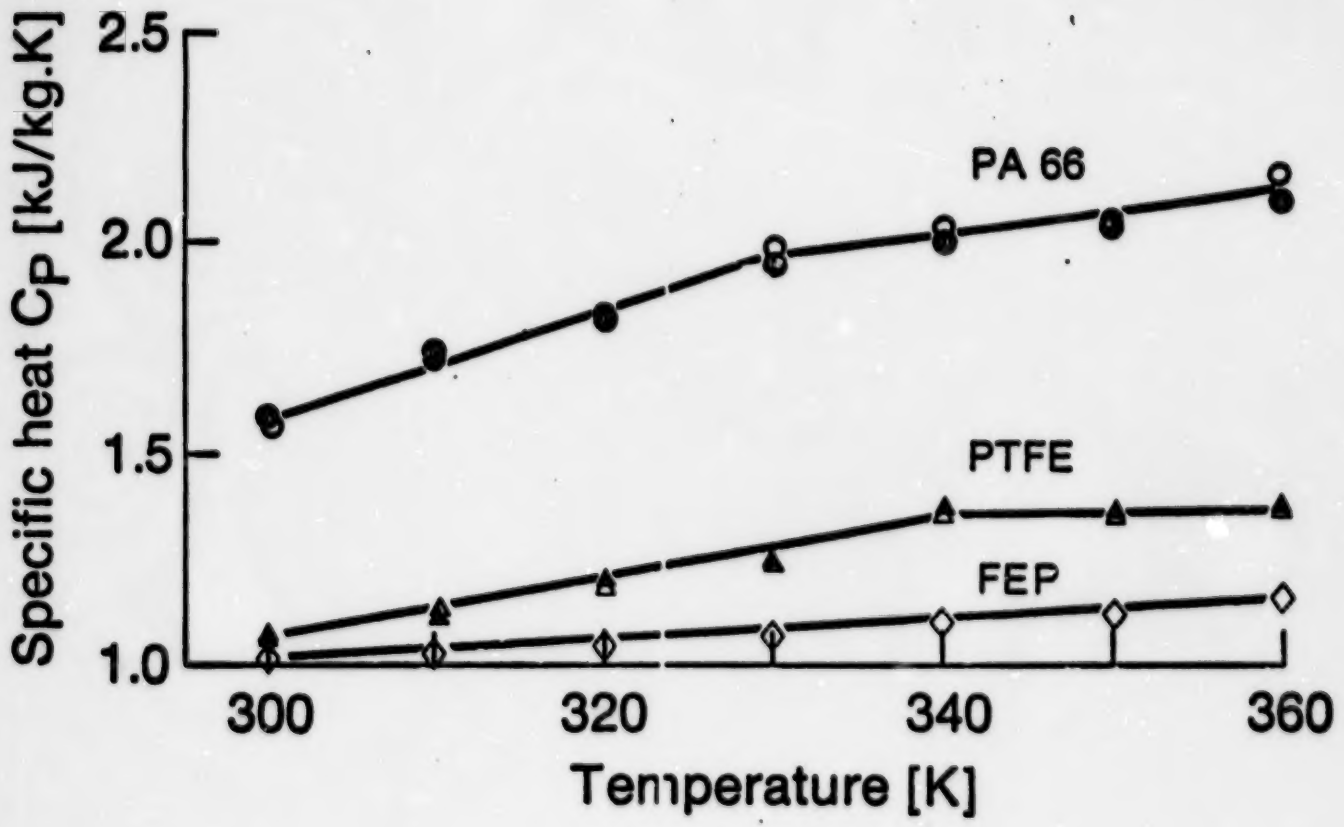
Specific heat C_P [kJ/kg.K]
2.5
2.0
1.5
1.0
PA 66
PTFE
FEP
300
320
340
360
Temperature [K]

Figure 2